

# Comparison Tools for Assessing the Microgravity Environment of Missions, Carriers and Conditions

Richard DeLombard and Kevin McPherson  
*Lewis Research Center*  
*Cleveland, Ohio*

Milton Moskowitz and Ken Hrovat  
*Tal-Cut, Company*  
*North Olmsted, Ohio*

April 1997



National Aeronautics and  
Space Administration

# **Comparison Tools for Assessing the Microgravity Environment of Missions, Carriers and Conditions**

Richard DeLombard  
Kevin McPherson  
*NASA Lewis Research Center  
Cleveland, Ohio*

Milton Moskowitz  
Ken Hrovat  
*Tal-Cut, Co.  
North Olmsted, Ohio*

April 1997

## Executive Summary

The Principal Component Spectral Analysis and the Quasi-steady Three-dimensional Histogram techniques provide the means to describe the microgravity acceleration environment of an entire mission on a single plot. This allows a straight forward comparison of the microgravity environment between missions, carriers, and conditions.

A Principal Component Spectral Analysis plot for the Life and Microgravity Sciences payload on the STS-78 mission in figure A illustrates the utility of this style of data presentation. Readily apparent are the two different acceleration levels resulting from the active and rest periods of the single shift crew during the mission. Equipment operated on that mission had a noticeable effect on the environment, as evidenced by the refrigerator/freezers and the Ku-band antenna system. Also apparent are the structural vibration mode frequencies of the Orbiter and the Spacelab module. The Principal Component Spectral Analysis technique is normally based on acceleration data with frequency content up to several hundred Hertz.

A Quasi-steady Three-dimensional Histogram plot for the STS-62 mission in figure B illustrates the utility of this style of data presentation. This data plot shows the different Orbiter flight attitudes as distinct clusters of data points. Three gravity gradient attitudes were used in a circular orbit which resulted in characteristics labelled as A, B and C in the data plot. Late in the mission, an elliptical orbit was used which resulted in the characteristics labelled as D in the data plot. The Quasi-steady Three-dimensional Histogram technique is normally based on acceleration data with frequency content below one Hertz.

This report shows that these techniques provide a tool for comparison between different sets of microgravity acceleration data, for example different missions, different activities within a mission, and/or different attitudes within a mission. These techniques, as well as others, may be employed in order to derive useful information from acceleration data.

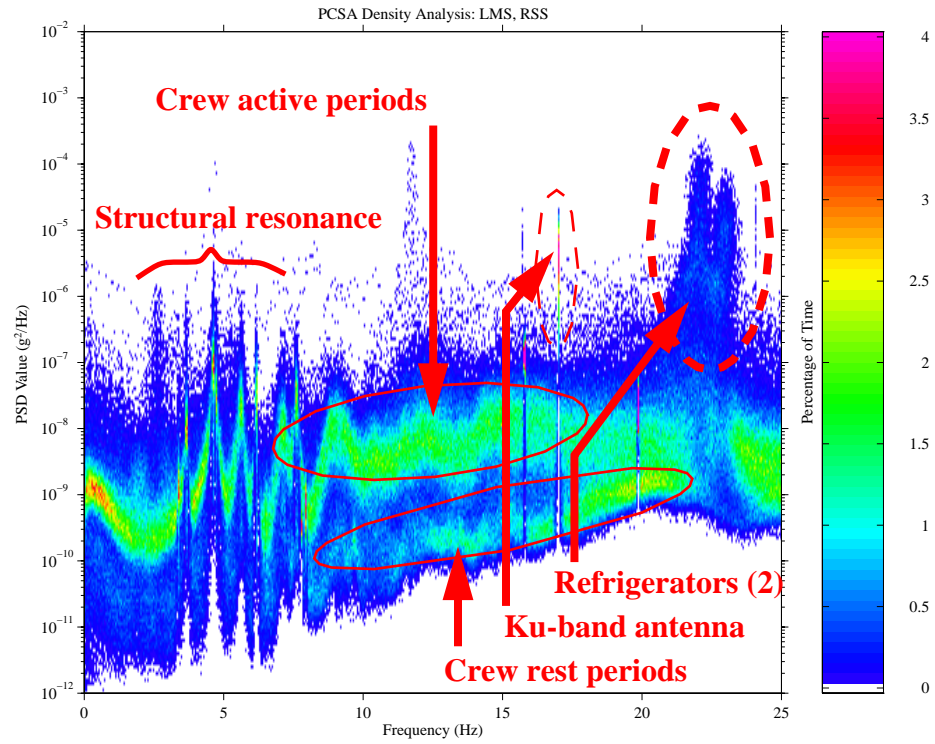


Figure A: Principal Component Spectral Analysis plot of SAMS data for STS-78.

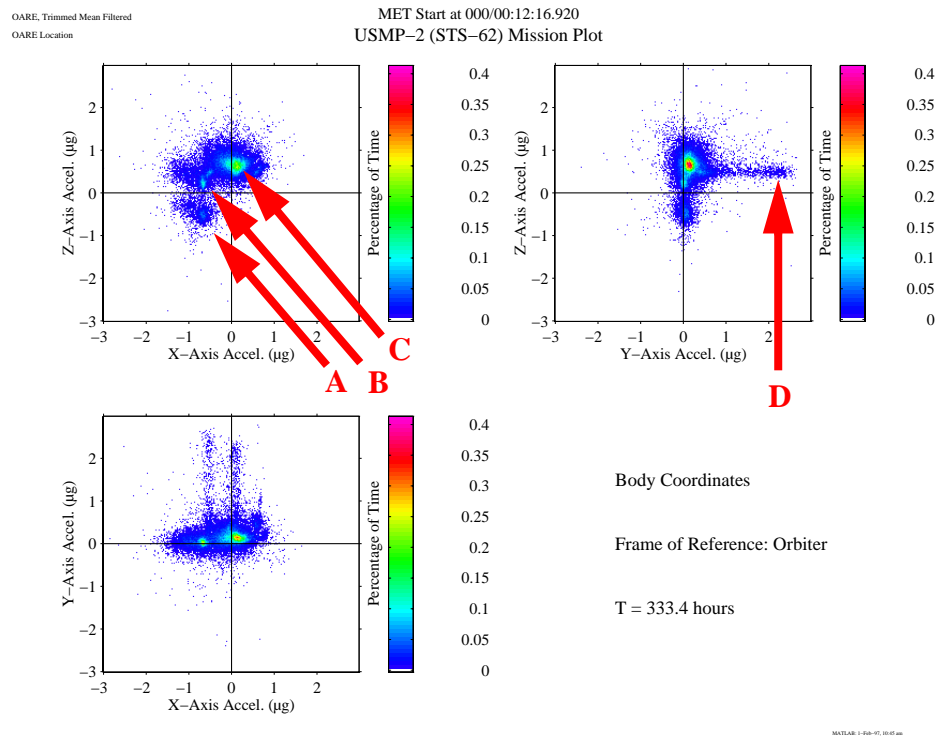


Figure B: Quasi-steady Three-dimensional Histogram plot of OARE data for STS-62.

# Table of Contents

Executive Summary .....	i
Table of Contents .....	v
List of Figures .....	vi
Acronym & Nomenclature List .....	vii
Introduction .....	1
Principal Component Spectral Analysis .....	1
PCSA Methodology .....	1
PCSA Interpretation .....	2
LMS / STS-78 Mission PCSA Characteristics .....	3
USML-1 / STS-50 Mission PCSA Characteristics .....	4
USMP-2 / STS-62 Mission PCSA Characteristics .....	4
USMP-3 / STS-75 Mission PCSA Characteristics .....	4
Mir Space Station PCSA Characteristics .....	5
PCSA Comparison .....	5
Quasi-steady Three-dimensional Histogram .....	6
QTH Methodology .....	6
QTH Interpretation .....	7
QTH Comparison .....	7
Microgravity Operations vs. Non-microgravity operations .....	7
Orbiter Altitudes .....	8
Orbiter Attitudes .....	8
Crew Activity .....	8
Future utilization .....	8
Conclusions .....	8
References .....	9

## List of Figures

A	Principal Component Spectral Analysis plot of SAMS data for STS-78.....	iii
B	Quasi-steady Three-dimensional Histogram plot of OARE data for STS-62. ....	iii
1	Sampled SAMS data set .....	10
2	Typical Power Spectral Density plot .....	11
3	Definition of a significant spectral peak .....	12
4	Extraction of spectral peaks from a portion of a typical Power Spectral Density plot .....	13
5	Typical Principal Component Spectral Analysis plot (STS-78 / LMS) .....	14
6	PCSA plot for STS-78 / LMS with typical PSD superimposed .....	15
7	PCSA plot for crew active on STS-78 / LMS mission .....	16
8	PCSA plot for crew rest on STS-78 / LMS mission .....	17
9	PCSA plot for STS-50 / USML-1.....	18
10	PCSA plot for USMP-2 microgravity portion of STS-62 .....	19
11	PCSA plot for USMP-3 microgravity portion of STS-75 .....	20
12	PCSA plot for crew active on Mir space station.....	21
13	PCSA plot for crew rest on Mir space station.....	22
14	OARE sampled data set in acceleration vs. time for STS-78 / LMS .....	23
15	Orbiter body axes coordinate system.....	24
16	Typical Quasi-steady Three-dimensional Histogram (STS-78 / LMS) .....	25
17	QTH plot for entire STS-62 mission .....	26
18	QTH plot for USMP-2 microgravity time of STS-62 .....	27
19	QTH plot during STS-62 with elliptical orbit parameters.....	28
20	QTH plot for -ZLV/+YVV attitude during STS-62 .....	29
21	QTH plot for -XLV/-ZVV attitude during STS-62 .....	30
22	QTH plot for -XLV/+ZVV attitude during STS-62 .....	31
23	QTH plot for crew active periods of STS-78 / LMS.....	32
24	QTH plot for crew rest periods of STS-78 /LMS .....	33

## Acronym & Nomenclature List

AIAA	American Institute of Aeronautics and Astronautics
$g_0$	normal Earth's gravity level at sea-level ( $\sim 9.81 \text{ m/s}^2$ )
LeRC	NASA Lewis Research Center
LMS	Life and Microgravity Sciences payload
LSLE	Life Sciences Laboratory Equipment
LV	local vertical
MET	Mission Elapsed Time
MPES	Mission Peculiar Equipment Support Structure
NASA	National Aeronautics and Space Administration
OARE	Orbital Acceleration Research Experiment
PCSA	Principal Component Spectral Analysis
PI	Principal Investigator
PIMS	Principal Investigator Microgravity Services
PSD	power spectral density
QTH	Quasi-steady Three-dimensional Histogram
SAMS	Space Acceleration Measurement System
STS	Space Transportation System
TM	Technical Memorandum
$\mu g$	$g_0 \times 10^{-6}$
USML	United States Microgravity Laboratory payload series
USMP	United States Microgravity Payload series
VV	velocity vector
$X_b, Y_b, Z_b$	Orbiter body coordinate system axes

## Introduction

The NASA Lewis Research Center (LeRC) manages several accelerometer projects for measuring the microgravity environment on board the NASA Orbiter missions and Russia's Mir space station, and, in the near future, free flyers and the International Space Station. These measurements and the subsequent analyses are performed in support of Principal Investigators (PIs) performing scientific experiments on these carriers.

The LeRC accelerometers currently operating on Orbiter missions are the Space Acceleration Measurement System (SAMS) [1, 2] and the Orbital Acceleration Research Experiment (OARE) instrument [3, 4]. In addition, one SAMS unit has been installed on the Mir space station. The SAMS measures the vibratory and transient environment from 0.01 Hz up to 100 Hz with a set of three distributed triaxial sensor heads. The OARE measures the quasi-steady environment below about 1 Hz near the Orbiter's center of mass.

The data sets from these instruments are analyzed by the NASA LeRC Principal Investigator Microgravity Services (PIMS) project and the results are provided to the PIs. After each mission with a SAMS and/or OARE instrument on board, the PIMS project prepares a summary report (e.g. [5, 6]) of the mission acceleration environment. These reports are provided to PIs for assistance during the analysis of their experimental data. The PIMS project also provides real-time and near-real-time analysis of the acceleration data during missions for which SAMS and/or OARE data are available via Orbiter downlink.

A number of standard formats for data display have been developed to illustrate the vast quantity of data acquired from the missions. Common formats are acceleration vs. time, power spectral density (PSD) vs. frequency, and spectrograms (PSD vs. frequency vs. time), illustrated in [7]. The particular technique used depends on the quantity of data considered, the requester's needs, and the type of information desired from the data plot. To analyze extensive periods of time these techniques result in many pages of plots.

There has been a need for a simple, integrated characterization of a mission, carrier, time period, etc. in order to compare this with another mission, carrier, time period, etc. An approach has been found by using the Principal Component Spectral Analysis (PCSA) and the Quasi-steady Three-dimensional Histogram (QTH) techniques. As will be shown in this report, the PCSA and QTH techniques bring both the range and median of the microgravity environment onto a single page for an entire mission or another time period or condition of interest. These single pages may then be used to compare similar analyses of other missions, time periods or conditions.

The PCSA plot is based on the frequency distribution of the vibrational energy and is normally used for an acceleration data set containing frequencies above the lowest natural frequencies of the vehicle (e.g. SAMS data). The QTH plot is based on the direction and magnitude of the acceleration and is normally used for acceleration data sets with frequency content less than 0.1 Hz (e.g. OARE data).

Various operating conditions are made evident by using PCSA and QTH plots. Equipment operating either full or part time with sufficient magnitude to be considered a disturbance is very evident as well as equipment contributing to the background acceleration environment. A source's magnitude and/or frequency variability is also evident by the source's appearance on a PCSA plot. The PCSA and QTH techniques are valuable tools for extracting useful information from acceleration data taken over large spans of time.

## Principal Component Spectral Analysis

### PCSA Methodology

The source of microgravity acceleration data for a PCSA plot is a sampled data set (figure 1) produced by an accelerometer system, such as SAMS. The time frame to be analyzed is first divided into successive equal-duration time intervals. The duration of an interval is chosen based upon the desired frequency resolution. The frequency resolution is given by  $\Delta f = 1/(\Delta t_i)$ , where  $\Delta f$  is the frequency resolution (in Hertz) and  $\Delta t_i$  is the length of time (in seconds) in each of the intervals. The PSD for each interval is

computed, figure 2.

The next step in the PCSA processing is to determine the significant spectral peaks in each of the PSDs from all of the successive time intervals. For the purpose of this discussion, a significant spectral peak (figure 3) is defined to be a PSD magnitude value that is a local maximum which is at least as high as any other magnitude point within a specified frequency range. The frequency range is usually specified by a number of frequency resolution intervals (a neighborhood) on either side of a data point. Typical values for this neighborhood are 0.05 - 0.10 Hz.

The magnitude and frequency of the significant spectral peaks are extracted from each individual PSD and stored as intermediate results (figure 4). From these sets of magnitude values versus frequency, a two-dimensional histogram is calculated by quantizing the magnitude and frequency to desired resolutions and assigning a count for each magnitude / frequency bin. A color is then assigned based on the number (count) of points falling within each of the magnitude / frequency bins. For the plots in this report, the magnitude resolution is logarithmic with the upper and lower magnitude bounds of the bins defined by  $10^{-N/20} g^2/Hz$ , for  $N = 40$  to  $240$ . This covers the upper and lower PSD magnitude bounds of  $10^{-2}$  and  $10^{-12} g^2/Hz$ .

The two-dimensional histogram calculation yields an array of the number of points falling within each magnitude / frequency bin. Therefore, the raw results of the histogram analysis are dependent on the total time period analyzed (e.g. 1 hour, or 10 days). A larger time period would be expected to result in a larger number of coincidences in any given bin. In order to counteract this time dependence, a normalization procedure is implemented by which the number of occurrences in any given bin are divided by the total number of periods analyzed for the plot. By doing this, a measure of the percentage of time is achieved by

the following equation:  $t_p = \frac{p}{M} \times 100\%$ , where  $t_p$  is the percentage of time,  $p$  is the number of points

falling within any given bin, and  $M$  is the number of periods analyzed for the PCSA plot. This data set is then imaged on a semi-log plot as in figure 5. This figure illustrates a PCSA plot for the SAMS data from the STS-78 mission which had the Life and Microgravity Spacelab (LMS) as the primary payload. Features of this data plot will be discussed in the next section.

The PCSA plots in this report have been plotted from zero to the filter cutoff frequency of the SAMS instrument. For the data shown in this report this cutoff frequency is 25 Hz unless specified otherwise.

## PCSA Interpretation

An individual set of significant spectral peak points extracted from a PSD indicate the upper levels of the microgravity environment for the time period of that particular PSD. This upper level of the microgravity environment is of interest to the vast majority of PIs for their analysis of the environment. For a complete PCSA plot, the range of the microgravity environment upper levels is bounded by the upper and lower edges of the color bands. Thus, with a single plot, the PCSA technique shows the range of the microgravity environment for that time period.

The PCSA technique is not useful for all analyses; for example, some PIs are concerned about acceleration levels in very narrow frequency bands. These PIs typically need data calculated for the root-mean-square levels of acceleration in frequency bands which affect their experiment apparatus. Different techniques typically used for acceleration data analyses are described in [7].

In this report, PCSA plots will be presented for several missions in order to show some of the characteristics discernible with the PCSA technique. The missions and pertinent characteristics are listed in table 1. Correlation of the PCSA plots with known mission events (e.g. Ku-band antenna dither) has led to a method to relate characteristics of a PCSA plot with mission activities and vehicle equipment operation. The basic interpretation of the plot's data is that the colors higher up the color bar scale (i.e. towards magenta) indicate that a magnitude/frequency combination occurred more often than that combination with a color lower on the scale. The bright band of reds/yellows/greens indicates the propensity of the microgravity environment to be in that region for much of the time included in the plot. This is illustrated in figure 5 where, for example, the tendency is for the environment below 1 Hz to be around  $10^{-9} g^2/Hz$ .

**Table 1: Example Missions and Characteristics**

MISSION	PRIMARY PAYLOAD	VEHICLE	CARRIER	CREW SHIFTS	OARE DATA
STS-50	USML-1	Orbiter	Spacelab module	2	yes
STS-62	USMP-2	Orbiter	MPESS	1	yes
STS-75	USMP-3	Orbiter	MPESS	2	yes
STS-78	LMS	Orbiter	Spacelab module	1	yes
Mir	multiple	Mir space station	Kvant, Kristal & Priroda modules	1	no

In figure 6, a typical PSD plot is superimposed on the PCSA plot of the STS-78 mission (from figure 5) to illustrate the relationship between PSD plots of microgravity acceleration data (which have been shown for years) and the PCSA plots. Notice that most of the PSD line follows one of the red/yellow/green areas described above. The PSD does not follow those areas for all frequencies, though, which illustrates the dynamic nature of the acceleration environment. This also points out a shortcoming in using a single PSD in order to represent the “typical” environment of a vehicle or mission.

Individual disturbances may be identified by certain characteristic shapes in a PCSA plot. The Ku-band antenna on the Orbiter dithers at a controlled 17 Hz rate to prevent mechanical stiction [6]. This fixed vibration rate produces the thin vertical line at 17 Hz in the PCSA plot for LMS (figure 5). The white area (representing very few histogram ‘hits’) below the 17 Hz thin vertical line means that the vibration at 17 Hz does not drop below  $2 \times 10^{-6} \text{ g}^2/\text{Hz}$  for any appreciable time in the mission. The conclusion drawn from this data is that the Ku-band antenna is operating for most, if not all of the mission, as it normally does for a mission of this nature where it is used for data downlink.

The well-known vehicle and payload structural vibration mode frequencies [8] are seen in a PCSA plot as the broad magnitude peaks in the lower frequency regions below 10 Hz. The Orbiter and its primary payload (e.g. Spacelab module) combine to produce a unique set of peaks for each mission at frequencies between 3 and 10 Hz, as seen in figure 5 (and others).

The unique characteristics present in the PCSA plots of several missions will be illustrated in the following subsections. Comparison of PCSA plots from different missions will then be shown in *PCSA Comparison*.

#### LMS / STS-78 Mission PCSA Characteristics

The LMS mission had a single shift crew which means that all seven crew members were on the same daily wake/sleep cycle. This mode of operation on the Orbiter produced two distinct microgravity environment characteristics. During the crew active time, equipment operation and crew motion contribute toward higher acceleration levels as compared with times for which the crew members were resting and sleeping. Crew active periods contribute to the higher magnitude disturbances seen in the LMS PCSA (figure 5) between  $10^{-7}$  and  $10^{-6} \text{ g}^2/\text{Hz}$  from about 8 to 21 Hz. Similarly, crew rest periods (reduced equipment operation and lack of crew motion) contribute to the lower microgravity levels between  $10^{-9}$  and  $10^{-7} \text{ g}^2/\text{Hz}$  in the same frequency band. To better illustrate this phenomenon, two days of SAMS data for LMS have been re-processed as two different plots; one (figure 7) for the time when the crew was active and the other (figure 8) for when the crew was sleeping. The separation of the microgravity levels is apparent in these two plots, especially in the 8 to 21 Hz range.

The two large “humps” in the LMS PCSA plot at around 22 and 23 Hz were caused by the two Life Sciences Laboratory Equipment (LSLE) refrigerator/freezers [9] located in rack 9 of the Spacelab module. These refrigerator/freezers operate with a motorized compressor/evaporator and the rotational speed and operating duty cycle vary according to the load and power supply characteristics. This produces a

vibration which varies in both magnitude and frequency, so the PCSA signature is not a tight frequency trace. For these two refrigerator/freezers, the vibrations produced by the motor/compressors was slightly different and they cycled on and off at regular but independent intervals during the course of the mission. Thus, there are times when the environment around 22 and 23 Hz is not dominated by the vibrations from one or both of these refrigerator/freezers. This results in histogram 'hits' below the  $10^{-5} \text{ g}^2/\text{Hz}$  level in that frequency range, as opposed to the white area at 17 Hz from the nearly constant dither of the Ku-band antenna.

The LMS mission had equipment which, when operated, produced vibrations at tightly controlled frequencies at just under 16 Hz and 20 Hz. The causes for these disturbances are not known at the present time. The source of the 16 Hz disturbance appears to have been on for most (but not all) of the mission. When on, it produced vibrations at the SAMS sensor head location at a level of  $10^{-5} \text{ g}^2/\text{Hz}$ , as evidenced by the short red line near 16 Hz in figure 5.

The source of the 20 Hz disturbance was active for nearly the entire mission, as evidenced by the white line at magnitudes lower than  $2 \times 10^{-7} \text{ g}^2/\text{Hz}$ . When on, it produced vibrations at the SAMS sensor head location of  $10^{-6} \text{ g}^2/\text{Hz}$ , as evidenced by the red line near 20 Hz in figure 5. There are times when other activities on the Orbiter increased the magnitude levels at this frequency. Recent research by the PIMS project indicates that this disturbance may be caused by the rotation of the SAMS optical disk drive. Testing accomplished during SAMS development indicated a 20 Hz vibration due to the disk drive motor rotation at 1200 revolutions per minute. The disturbance signal has been seen in other methods of data display (i.e. PSD, spectrogram) but was quite often masked by other disturbances. The PCSA plot clearly shows the presence of the disturbance even though other disturbances mask it. This disturbance is seen in the other mission PCSA plots in this report, including the PCSA plots of the Mir data.

#### USML-1 / STS-50 Mission PCSA Characteristics

The primary payload on this mission was the First U. S. Microgravity Laboratory (USML-1). This mission had a dual crew shift throughout the mission. The PCSA plot for this mission (figure 9) exhibits a single level as opposed to the two levels seen on a single crew shift mission, such as LMS (figure 5). This is indicative of the two crew shifts, thus keeping activity at similar levels throughout the mission.

There were equipment operations which produced vibrations at about 12.5, 20, and 21 Hz, none of which appeared to be on for the entire mission. The causes for these disturbances are not known at the present time.

A LSLE refrigerator / freezer was not flown on this mission, and the data do not show the peaks at about 22 Hz which are normally caused by this equipment.

#### USMP-2 / STS-62 Mission PCSA Characteristics

One of the primary payloads on this mission was the Second U. S. Microgravity Payload (USMP-2). A PCSA plot for the USMP-2 payload microgravity time on the STS-62 mission is shown in figure 10. This mission had a single crew shift and the PCSA plot exhibits the two basic magnitude levels between 10 Hz and 15 Hz associated with crew active and crew quiet time periods. This is similar to the characteristics described above for the LMS payload on the STS-78 mission.

There are also several unique disturbances in the 15 Hz to 21 Hz region. The causes for these disturbances are not known at the present time, except for the 17 Hz signal attributed to the Ku-band antenna, as described above.

The faint "clusters" of points in the 1.25 Hz and 2.5 Hz region with magnitudes between  $10^{-7}$  and  $10^{-5} \text{ g}^2/\text{Hz}$  appear to be due to crew exercise [6] on an ergometer. The two frequencies arise from the crew members' body motions and pedaling rates.

#### USMP-3 / STS-75 Mission PCSA Characteristics

A PCSA plot for the USMP-3 payload microgravity time on the STS-75 mission is shown in figure 11. This mission had two crew shifts and the PCSA plot exhibits a single predominate magnitude characteristic associated with nearly constant crew activity throughout the mission. This is similar to the

USML-1 mission characteristics described above.

Other disturbance sources are evident in the 19 Hz to 21 Hz region. Once again, the causes for these disturbances are not known at the present time.

### Mir Space Station PCSA Characteristics

PCSA plots from some of the SAMS data collected in the Priroda module of the Mir space station are in figures 12 and 13. Additional characterization of the Mir microgravity environment is contained in [10, 11, 12, 13].

Figure 12 illustrates the microgravity environment for three days of time while the crew members were active; figure 13 is for the corresponding time while the crew members were sleeping. Similar to the appearance of the PCSA plot for the LMS mission, there is a marked difference between these two conditions.

The more consistent magnitude levels of acceleration during crew rest are evident in comparing the magnitude variability of the color areas of figures 12 and 13. For a particular frequency, the magnitude variation is less for the crew rest time than during the crew active time.

Russia's Mir space station has lower natural structural frequencies and its peaks range from below 1 Hz up to 5 Hz as seen in figures 12 and 13. This is comparable with similar characteristics (but different frequencies) of the Orbiter mission data.

Notice that the disturbance just below 20 Hz appears in the SAMS data from Mir also. Since there are very few pieces of U.S. equipment on Mir, the presence of this disturbance lends credence that this disturbance is due to the SAMS optical disk drive (see section *LMS / STS-78 Mission PCSA Characteristics*).

Note that the data in figures 12 and 13 have a frequency cutoff of 100 Hz and a sampling rate of 500 samples per second. These PCSA plots have been prepared to include only 25 Hz for ready comparison with the other PCSA plots in this report.

## **PCSA Comparison**

There have been many situations in the past where a user has asked the PIMS project to prepare a comparison of a period of time from one mission with a period of time from either the same or a different mission. Such a comparison is not reasonable to perform by using standard PSD plots because the microgravity acceleration environment is so dynamic. Comparison of long-duration PSDs is hindered by the non-stationary nature of the acceleration environment. Spectral averaging techniques intended to suppress spurious peaks and accentuate significant spectral contributions obscure the spectrum where brief, transitory contributions occur. Selecting data from a "representative" time is another complicating factor when trying to utilize standard PSD plots to illustrate the general microgravity environment.

A PCSA plot allows the user to make a visual comparison between missions, carriers (e.g. the Spacelab module and the Orbiter's middeck), time periods within a mission (e.g. crew active and crew sleep) and mission conditions (e.g. different Orbiter attitudes, different levels of crew activity, etc.). Timing information has been removed by the processing to arrive at a PCSA plot, but this technique provides the desired comparison with respect to the overall magnitude levels and trends.

As discussed earlier, figures 7 and 8 provide a comparison of the LMS environment for when the crew was active and when the crew was sleeping. The separation of the microgravity levels is apparent in these two plots, especially in the 8 to 20 Hz range. In practice, this technique may be used to assist in the operations planning of microgravity science experiments which are sensitive to acceleration disturbances. This type of plot may be used to show the PI that the crew sleep period has a reduced microgravity level in the frequency range of concern and, therefore, operation of the experiment for the hours during crew rest would be more advantageous.

The PCSA plots from two Spacelab module missions, LMS (a single shift crew) and USML-1 (a dual shift crew), may be compared by examining figures 5 and 9, respectively. The predominant PSD magnitude levels of the USML-1 mission are comparable with the PSD magnitude levels from the crew active traces seen in the LMS PCSA plot.

Missions with single shift crews but with different payload carriers (LMS with a Spacelab module and USMP-2 with a Spacelab Mission Peculiar Equipment Support Structure (MPRESS)), may be compared by examining figures 5 and 10, respectively. The crew active times during LMS are slightly higher in magnitude between 5 and 20 Hz, whereas the levels were more comparable during the crew rest times. There appears to be more structural natural vibration modes for LMS with the Spacelab module than there were for USMP-2 with the MPRESS carrier.

Two missions with Spacelab MPRESS carriers but with different crew activity schedules (USMP-2 with a single crew shift and USMP-3 with a dual crew shift), may be compared by examining figures 10 and 11, respectively. It is interesting to note that the predominant levels for USMP-3 are comparable to the crew rest times of USMP-2, even though USMP-3 was a dual crew shift mission and USMP-2 had a single crew shift. This seems to corroborate that the crew of USMP-3 were consciously attempting to work quietly during the microgravity experimentation period. When discussing the use of the acceleration data display for the STS-75 crew, Franklin Chang-Diaz, the Payload Commander, said

*“The application was easy to use and useful for crew feedback. It influenced our activities greatly and made us much more aware of the potential crew-induced disturbances. It is a great on-orbit training tool for crews to develop an efficient low-g way of doing things. It also shows that we can do effective work without interfering with micro-g operations...”* [14]

Missions with single shift crews but with vastly different vehicles (LMS with a Spacelab module on the Orbiter Columbia and the Priroda module on the Mir space station) may be compared by examining figures 5 and 12, respectively.

The varied equipment used on the different vehicles produce disturbances at different frequencies and magnitudes as seen in figures 5, 12 and 13 and explained in previous sections.

## **Quasi-steady Three-dimensional Histogram**

### **QTH Methodology**

The source of microgravity acceleration data for a QTH plot is a sampled data set produced by a low frequency accelerometer system, such as the OARE. The OARE data for the LMS mission are shown in figure 14.

The original OARE data are acceleration measurements digitized at a rate of 10 samples per second for each of the X, Y, and Z axes. Prior to its use in QTH plots, the data are transformed from the OARE coordinate system to the Orbiter body coordinate system (figure 15 and reference [7]) and a trimmed-mean filter is applied to the data [3, 4]. The trimmed-mean filter is used to gain a better estimate of the quasi-steady acceleration levels. The filtering procedure ranks the collected data in order of increasing magnitude, measures the deviation of the distribution from a normal distribution, and deletes (trims) an adaptively determined amount of the data. The mean of the remaining data is calculated and this value is assigned to the initial time of the interval analyzed. For this report, the filter was applied to 50 seconds (500 sampled data points) of OARE data in order to generate a data point every 25 seconds.

From these sets of three-axis magnitude values, three two-dimensional histograms are formed by plotting pairs of the three-axis data points in three scatter diagrams (figure 16). These three diagrams provide front, side, and top views of the acceleration vectors. The histogram is calculated by quantizing the magnitudes to a desired resolution and assigning a count for an occurrence in each bin. A color is then assigned based on the number of occurrences that fall within each bin. For the QTH plots in this report, the magnitude is linear with a range of  $\pm 2 \mu g$ , unless otherwise noted.

The two-dimensional histogram calculation yields a matrix of the number of points falling within each histogram bin. Therefore, the raw results of the histogram analysis are dependent on the total time period analyzed (e.g. 1 hour, or 10 days). A larger time period would be expected to result in a larger number of coincidences in any given bin. In order to counteract this time dependence, a normalization procedure is implemented by which the number of occurrences in each bin is divided by the total number of periods analyzed for the plot. By doing this, a measure of the percentage of time is achieved by the following

equation:  $t_p = \frac{p}{N} \times 100 \%$ , where  $t_p$  is the percentage of time,  $p$  is the number of points falling within a bin, and  $N$  is the number of data points included in the QTH plot analysis.

This data set is then imaged as the three scatter plots in figure 16. The axis origin is centered on the OARE instrument sensor's location. As acceleration data, a QTH data point should be viewed as the tip of a vector with an origin at the OARE sensor. The location of the data point in the QTH then gives a relative indication of the quasi-steady acceleration vector magnitude and direction.

The OARE data from a mission may also be transformed to different locations on the Orbiter by incorporating the Orbiter state vector data. These transformed data may then be used to prepare a QTH plot to indicate the quasi-steady conditions at an experiment location or any other position of interest.

## QTH Interpretation

For this paper, several missions will be illustrated with QTH plots to show some of the characteristics discernible with this technique. The only long-term quasi-steady data available from multiple missions is from the OARE instrument. The OARE instrument has only been flown on the Orbiter Columbia and thus limiting this form of analysis to just some of the microgravity missions. The QTH plots in this report are presented in terms of the Orbiter body coordinate system [7] and thus are directly comparable with one another. The sign convention is based on the acceleration of free floating particles within the vehicle [7].

Correlation of the QTH plots with known mission events (e.g. Orbiter attitudes, water dumps) has led to the interpretation of the QTH plot characteristics relative to mission activities and vehicle equipment operation. The basic interpretation of the plot's data is that the colors higher up the color-bar scale (toward magenta) indicate that the acceleration vector fell into that bin more often than those bins with a color lower on the scale. The bright area of reds/magentas indicate the propensity of the microgravity environment to be in that region for most of the time of the data included in the plot. This is illustrated in figure 16, where the tendency for the quasi-steady acceleration vector to be either near  $(X_b, Y_b, Z_b) = (-0.1, -0.1, 0.5) \mu\text{g}$  or near  $(-0.6, -0.1, 0.3) \mu\text{g}$ . The two regions are due to the two principal attitudes of the Orbiter for this mission, as explained in *Orbiter Attitudes*, below.

The general range of microgravity environment conditions for the time of the data included in a QTH plot is bounded by the extent of the colored areas in the plot. Due to the processing used, there may be individual points outside the colored areas, though. The QTH plot indicates the propensity (if any) of the quasi-steady acceleration vector direction and magnitude over the time period included in the plot.

## QTH Comparison

There have been many situations in the past where a user has asked the PIMS project to prepare a comparison of the quasi-steady conditions for a long period of time in a mission with another period of time in the same mission or for a comparison between missions. Such comparisons using plots of acceleration versus time are not adequate because the microgravity quasi-steady acceleration levels slowly change over time. The overall conditions are not readily apparent.

The QTH plot allows the user to make a visual comparison between missions, carriers, time periods of a given mission, and conditions (i.e. attitudes, crew activity, etc.) by showing long-duration changes in the quasi-steady acceleration environment in a single plot.

### Microgravity Operations vs. Non-microgravity operations

The first nine days of the STS-62 mission were devoted to operations for the USMP-2 payload while the last five days were devoted to the OAST-2 payload [6]. The difference in the quasi-steady acceleration environment is easily seen by comparing figure 17, which includes the entire mission, and figure 18, which includes only the USMP-2 microgravity operations time. Note the scales in these figures are  $\pm 3 \mu\text{g}$ . The primary causes for the differences between parts of the same mission are the Orbiter attitudes and altitudes, Orbiter motion, and increased crew activity which occurred during the OAST-2 payload operations.

### Orbiter Attitudes

During the OAST-2 payload operations of the STS-62 mission [6], the Orbiter operated in the -ZLV/+YVV attitude in an elliptical orbit with altitudes of 105 nautical miles (perigee) and 138 nautical miles (apogee). The QTH for this type of orbit is shown in figure 19. Note the scales in this figure are  $\pm 3 \mu g$ . The acceleration levels in the data plot are such that the increased drag at the lower altitudes increased the acceleration levels in the axis directed into the velocity vector (the  $Y_b$  axis in this case).

### Orbiter Attitudes

The main Orbiter attitudes utilized during the microgravity portion of STS-62 were described in general in [7] and more specifically in the PIMS mission summary report for STS-62 [6]. Three of the attitudes were -ZLV/+YVV (cargo bay to Earth, right wing forward), -XLV/-ZVV (tail to Earth, cargo bay forward), and -XLV/+ZVV (tail to Earth, belly forward). Individual QTH plots for these three attitudes are shown in figures 20 to 22, respectively. The predominant direction of the quasi-steady acceleration may be seen where the colored area is red/magenta. Each attitude's contribution to the mission QTH plot may be seen by comparing figures 20, 21, and 22 with figure 18.

### Crew Activity

Figure 14 contains the OARE data from the entire STS-78 mission plotted as acceleration versus time. An explanation of the microgravity environment of this mission is in the *LMS / STS-78 Mission PCSA Characteristics* section and in [9]. The salient points from this figure are the regular crew active and crew rest periods. The crew active times are evident from the increased levels of acceleration for about 18 hours every day, such as between Mission Elapsed Time (MET) hours 42 and 60. The crew rest times are evident from the times with little scatter in the data, such as around hour 65. QTH plots containing three crew active periods and three crew rest periods are shown in figures 23 and 24, respectively.

Some experiments require a steady direction and magnitude of the quasi-steady acceleration vector during the experiment operations. This analysis of crew active and rest periods shows that it would be more advantageous to operate experiments which are sensitive to acceleration magnitude and/or direction changes during the crew rest periods.

## **Future utilization**

The PCSA and QTH plots are useful during the analysis of the vast quantity of data which is currently being received from SAMS operations on Orbiter missions and the Mir space station. Even more so, these techniques will be useful for analyzing the data from the SAMS unit for the International Space Station operations.

These techniques may also be used as a calculation technique in a neural network data interpretation system under development by PIMS. Processing the mission data using these techniques will allow a neural network system to recognize the mission activities described in this paper.

## **Conclusions**

The PCSA and QTH plots provide tools with which to compare different sets of microgravity acceleration data. These techniques, as well as others, may be employed in the analysis of acceleration data from microgravity science missions in order to derive useful information in support of the microgravity science experiments.

## References

1. DeLombard, R. and Finley, B.D.: Space Acceleration Measurement System Description and Operation on the First Spacelab Life Sciences Mission, NASA TM-105301, 1991.
2. DeLombard, R.; Finley, B.D.; and Baugher, C.R.: Development of and Flight Results from the Space Acceleration Measurement System (SAMS), AIAA 92-0354 (NASA TM-105652), January 1992.
3. Blanchard, R. C.; Hendrix, M. K.; Fox, J. C.; Thomas, D. J.; and Nicholson, J. Y.: Orbital Acceleration Research Experiment. *Journal of Spacecraft and Rockets*, Vol. 24, No. 6, 1987.
4. Blanchard, R. C.; Nicholson, J. Y. and Ritter, J. R.: STS-40 Orbital Acceleration Research Experiment Flight Results During a Typical Sleep Period, *Microgravity Science Technology*, Vol. V, No. 2, 1992.
5. Rogers, M. J. B. and DeLombard, R.: Summary Report of Mission Acceleration Measurements for STS-65, NASA TM-106871, 1995
6. Rogers, M. J. B. and DeLombard, R.: Summary Report of Mission Acceleration Measurements for STS-62, NASA TM-106773, 1994
7. DeLombard, R.: Compendium of Information for Interpreting the Microgravity Environment of the Orbiter Spacecraft, NASA TM-107032, 1996.
8. Nelson, E. S.: An Examination of Anticipated g-Jitter on Space Station and Its Effects on materials Processes, NASA TM-103775, May 1991
9. Hakimzadeh, R.; Hrovat, K.; McPherson, K. M.; Moskowitz, M.; and Rogers, M. J. B.: Summary Report of Mission Acceleration Measurements for STS-78, NASA TM-107401, 1997
10. DeLombard, R. and Rogers, M. J. B.: Quick Look Report of Acceleration Measurements on Mir Space Station During Mir-16, NASA TM-106835, 1995
11. DeLombard, R.; Ryaboukha, S. (RSC Energia); Hrovat, K.; and Moskowitz, M.: Further Analysis of the Microgravity Environment on Mir Space Station During Mir-16, NASA TM-107239, 1996
12. DeLombard, R.; Hrovat, K.; Moskowitz, M.; and McPherson, K.: SAMS Acceleration Measurements on Mir From June to November 1995, NASA TM-107312, 1996
13. DeLombard, R.: SAMS Acceleration Measurements on Mir From November 1995 to June 1996, NASA TM-107435, 1997
14. Rogers, M. J. B.; Hrovat, K.; Moskowitz, M. E.; McPherson, K; and DeLombard, R.: Summary Report of Mission Acceleration Measurements for STS-75, NASA TM-107359, 1996

Figure 1: Sampled SAMS data set  
(acceleration vs. time)

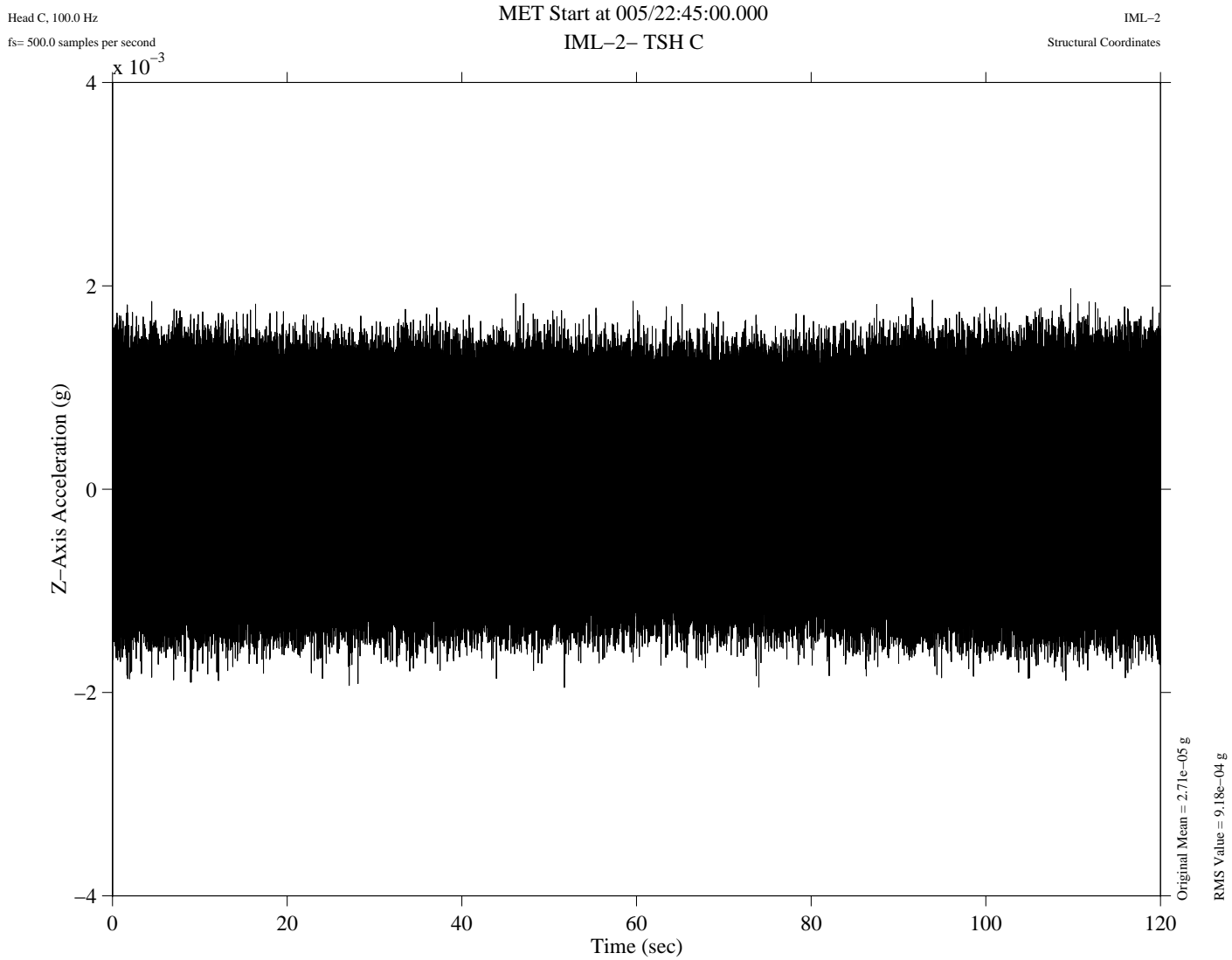
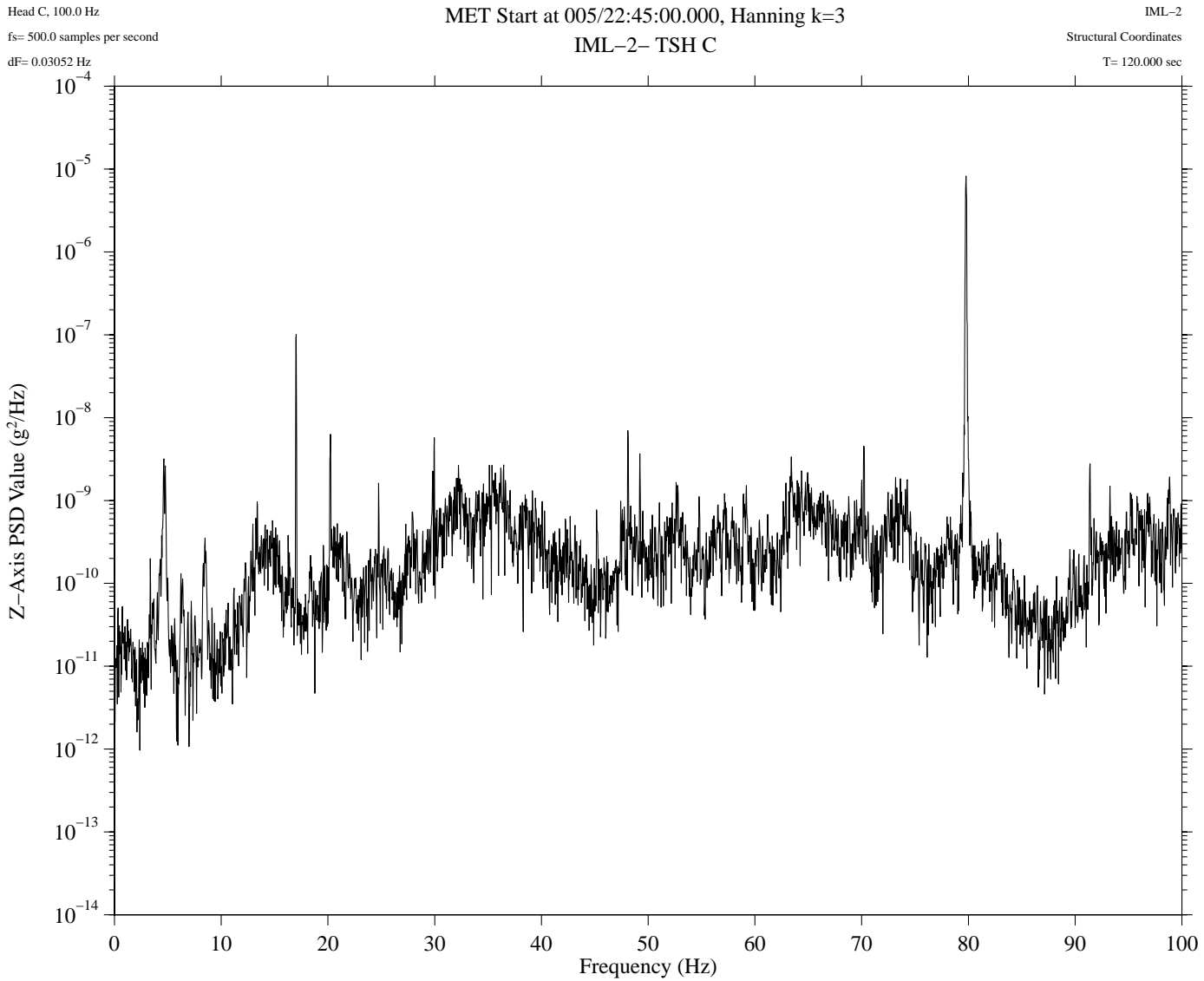


Figure 2: Typical Power Spectral Density plot  
(magnitude vs. frequency)



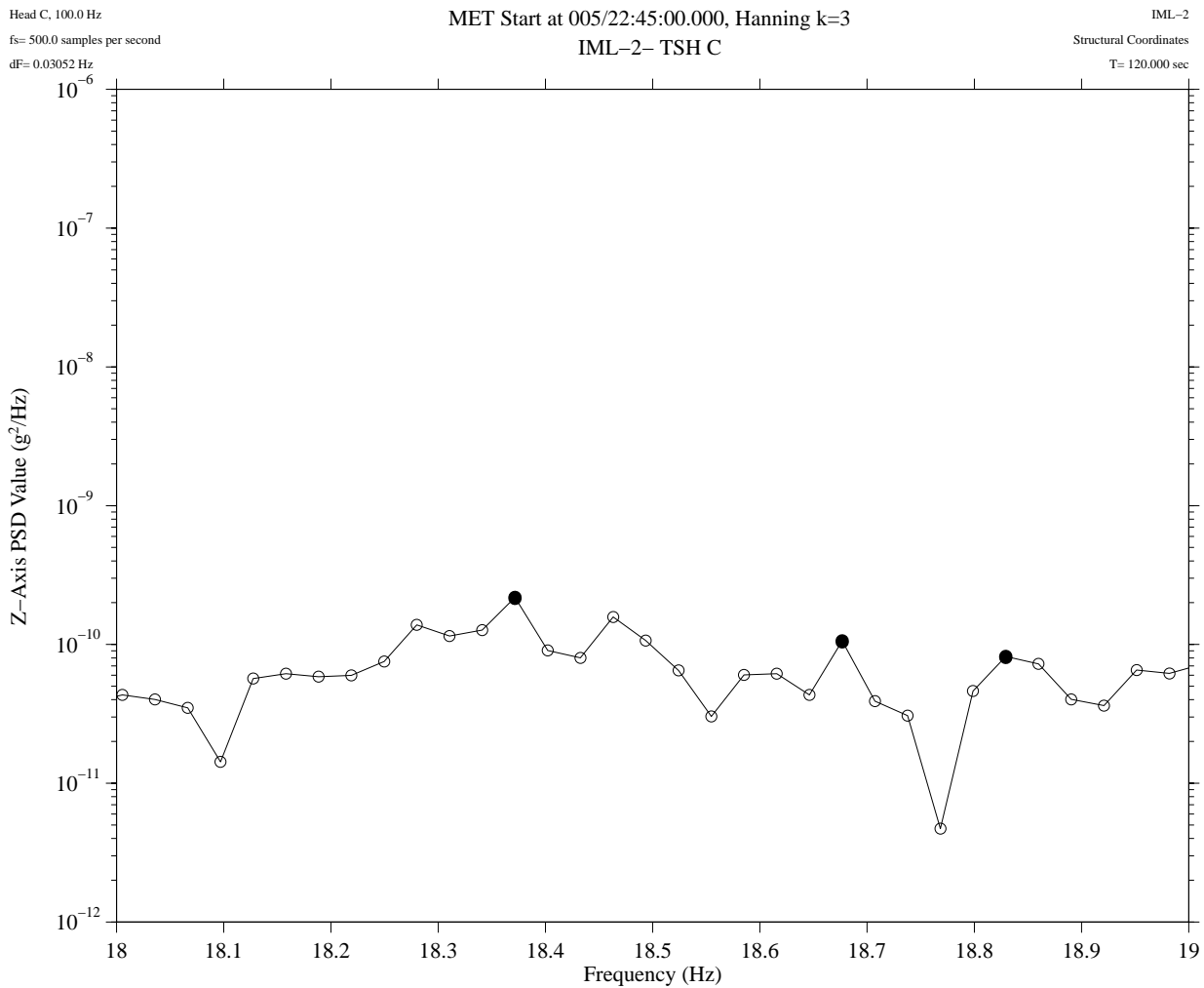


Figure 3: Definition of a significant spectral peak  
 (circles are individual data points and solid circles are significant spectral peaks)

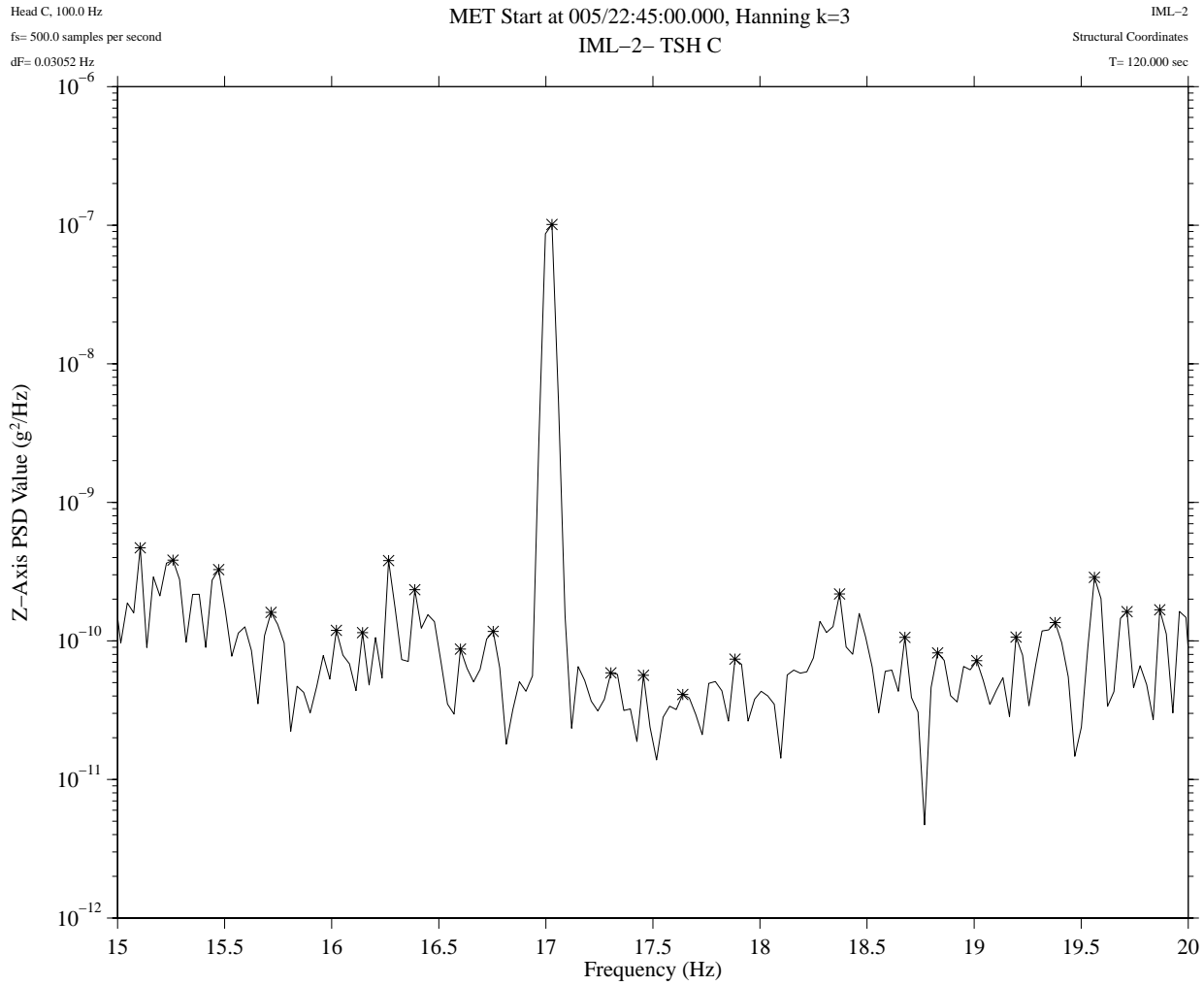


Figure 4: Extraction of spectral peaks from a portion of a typical Power Spectral Density plot

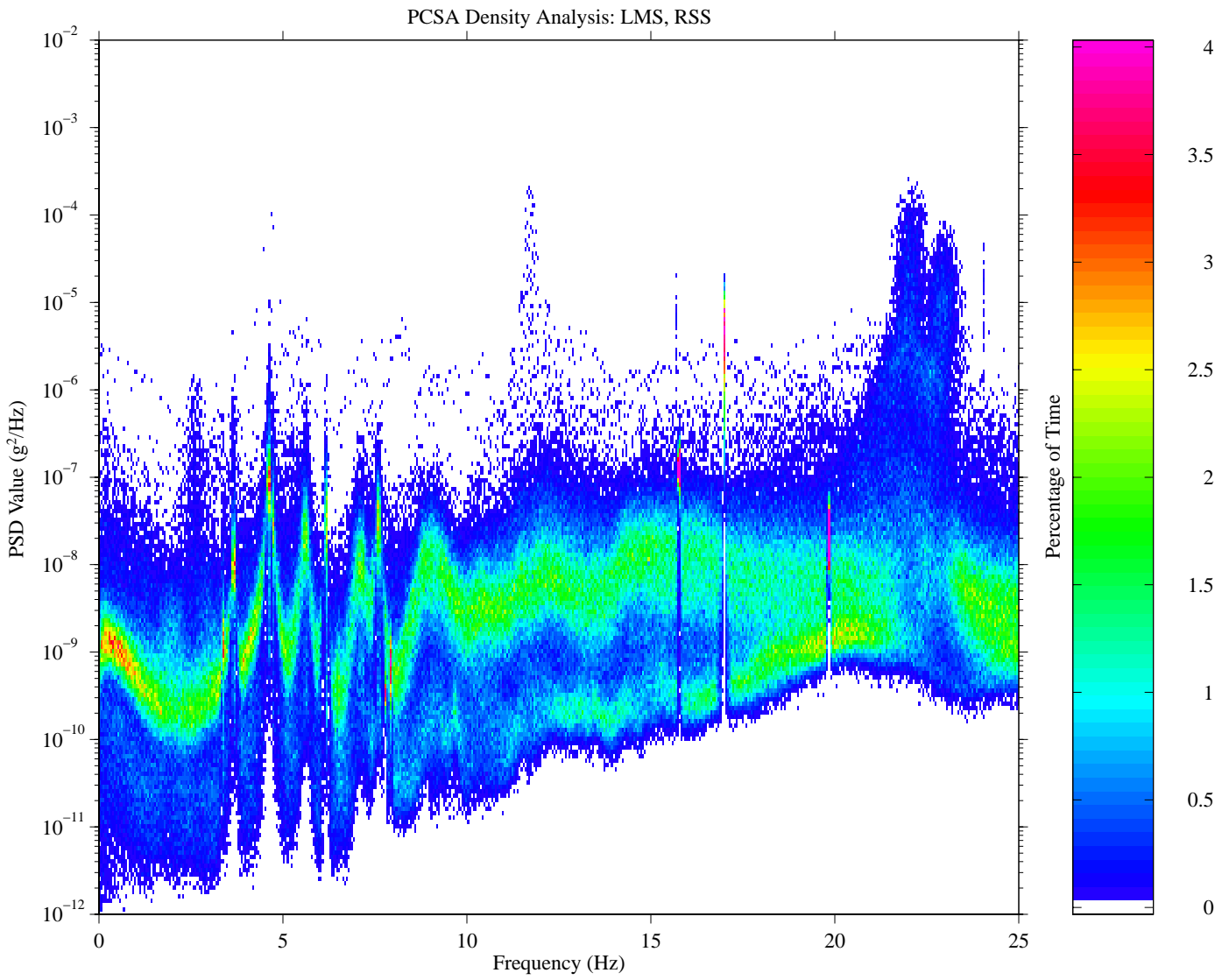


Figure 5: Typical Principal Component Spectral Analysis plot (STS-78 / LMS)

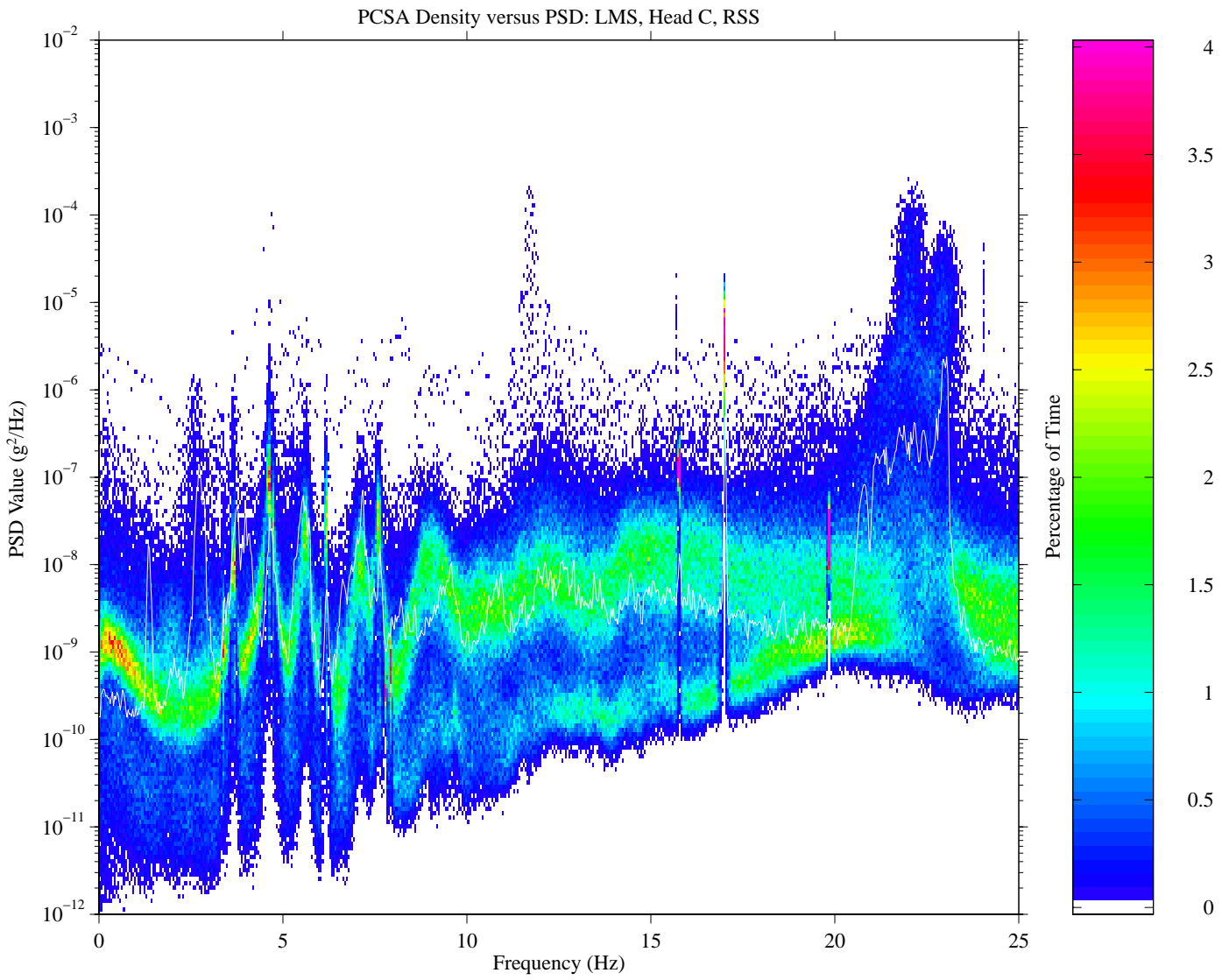


Figure 6: PCSA plot for STS-78 / LMS with typical PSD superimposed

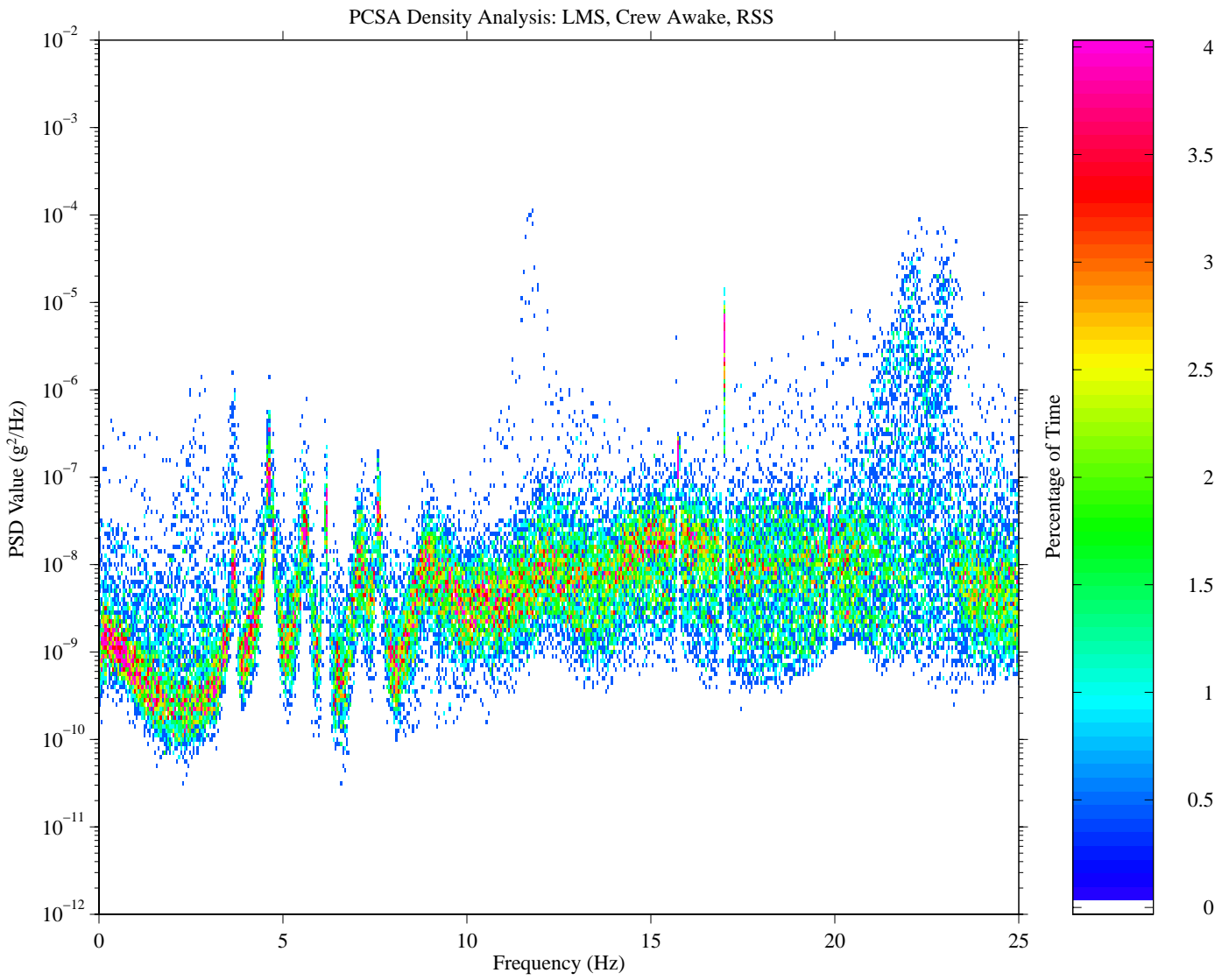


Figure 7: PCSA plot for crew active on STS-78 / LMS mission

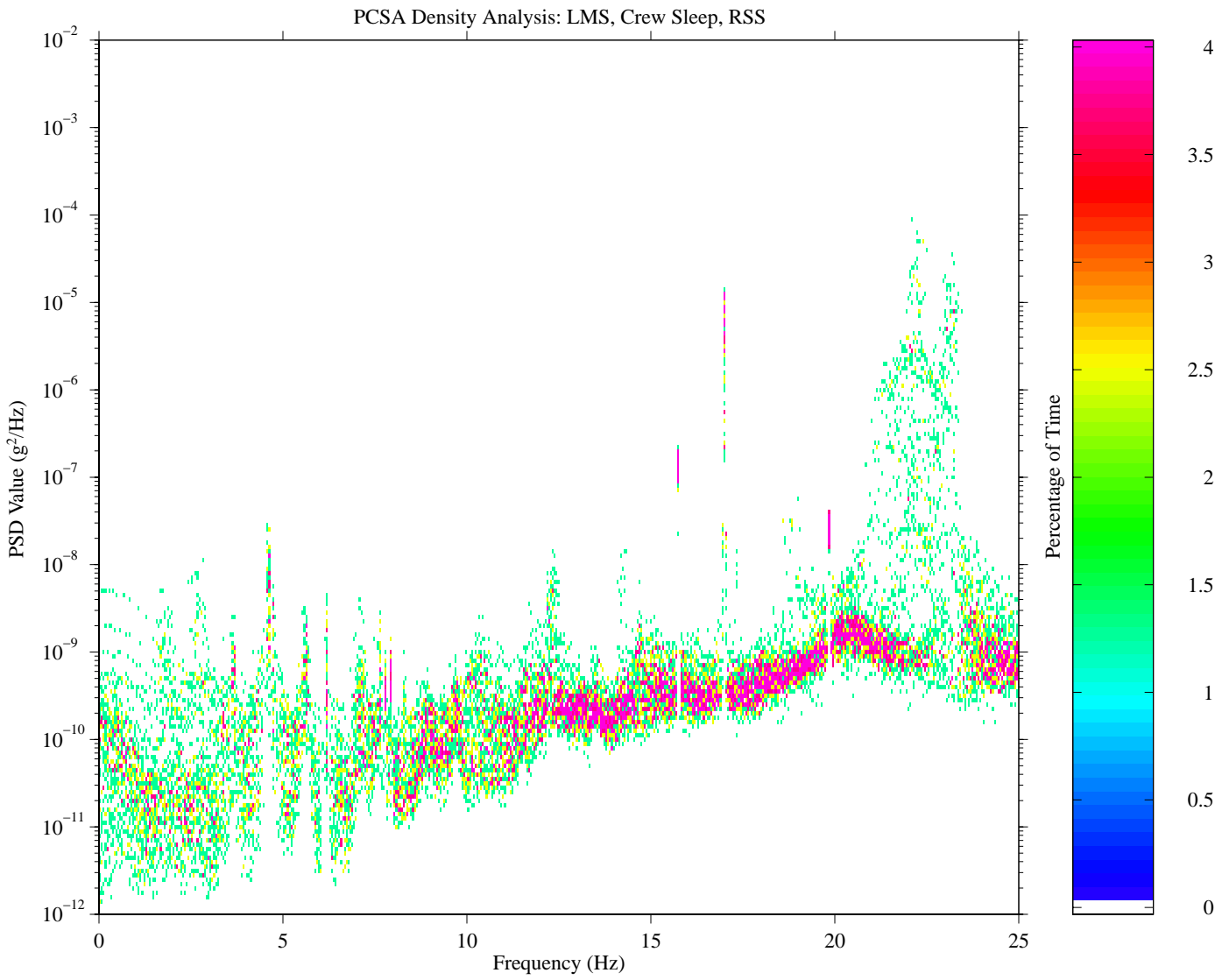


Figure 8: PCSA plot for crew rest on STS-78 / LMS mission

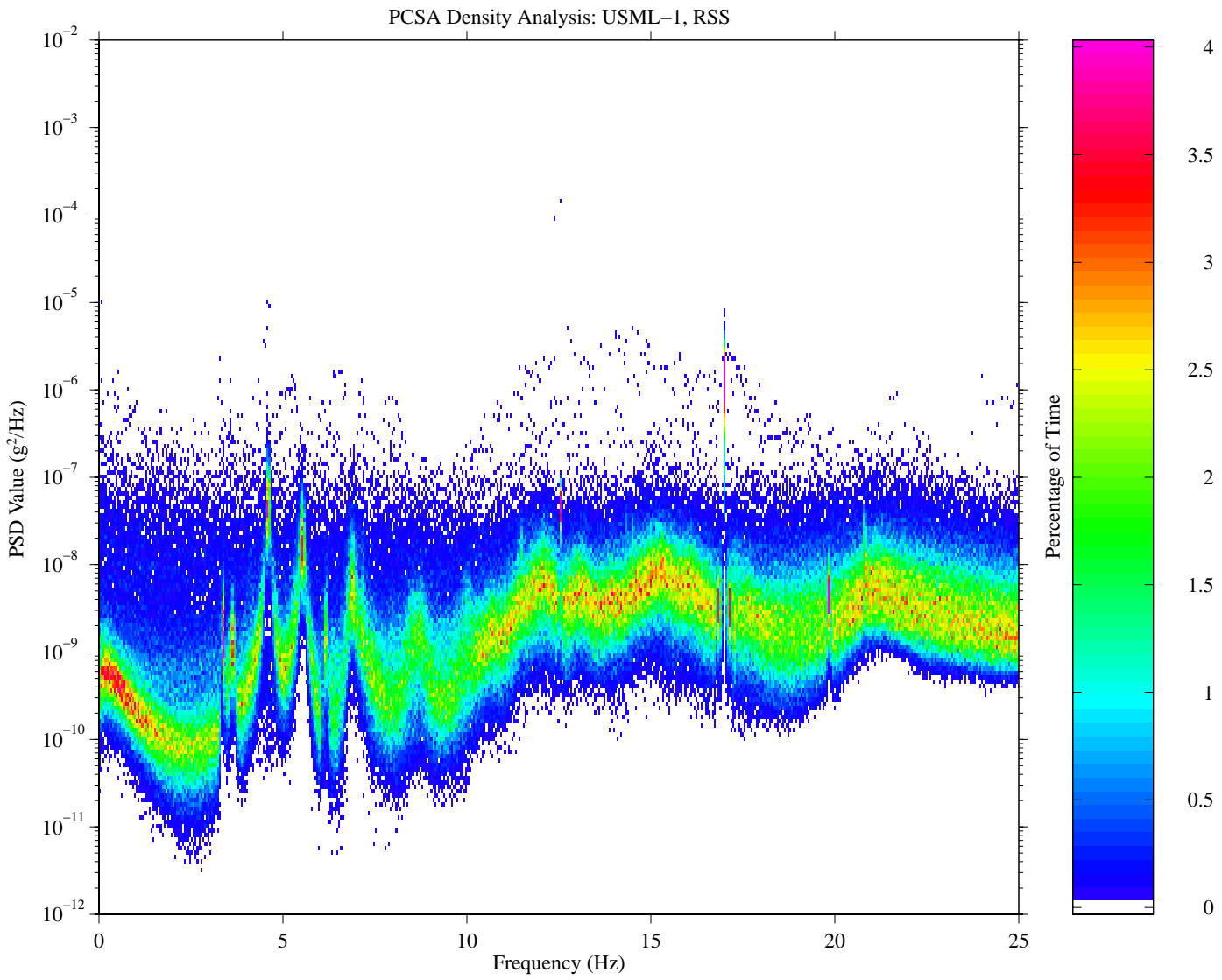


Figure 9: PCSA plot for STS-50 / USML-1

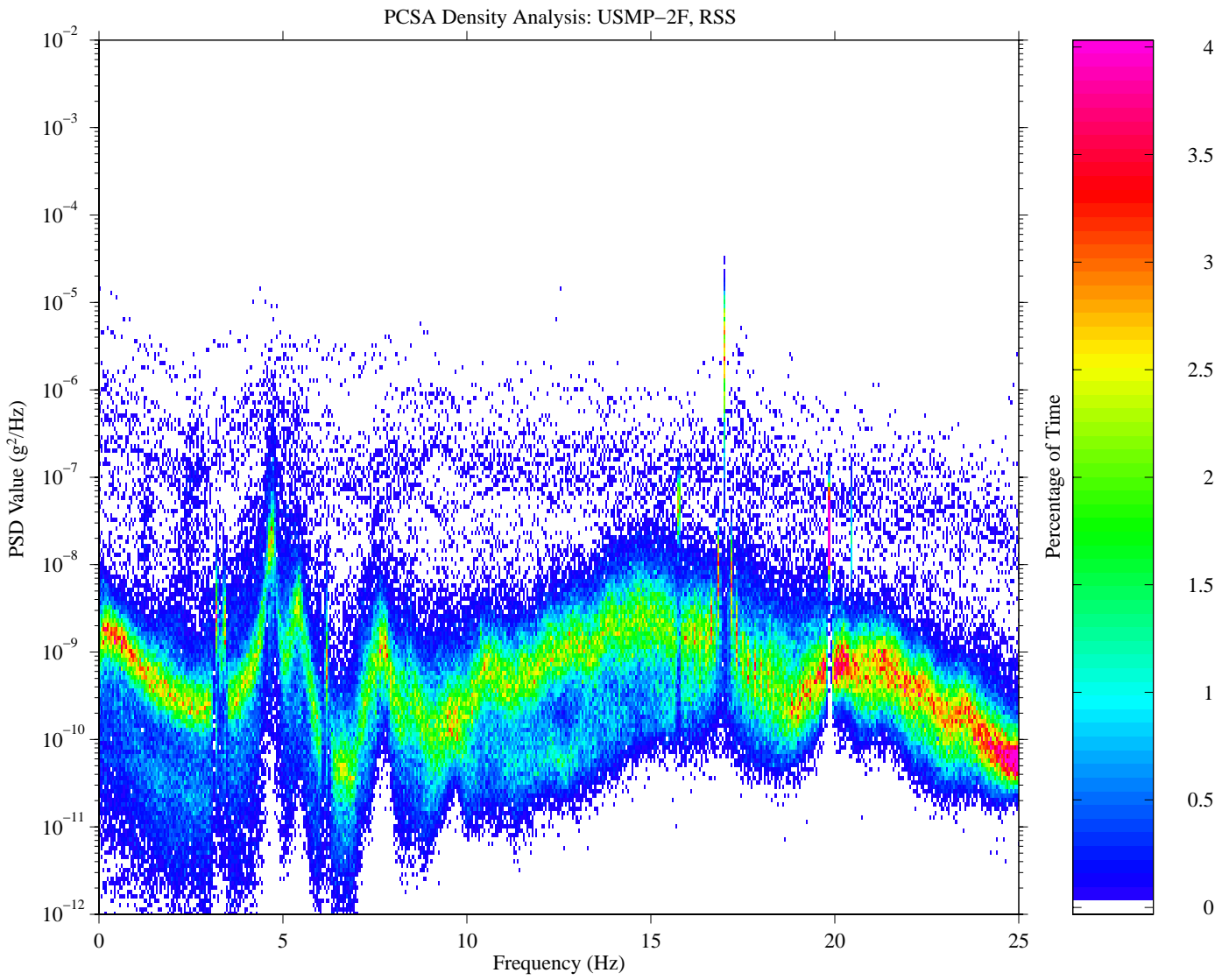


Figure 10: PCSA plot for USMP-2 microgravity portion of STS-62

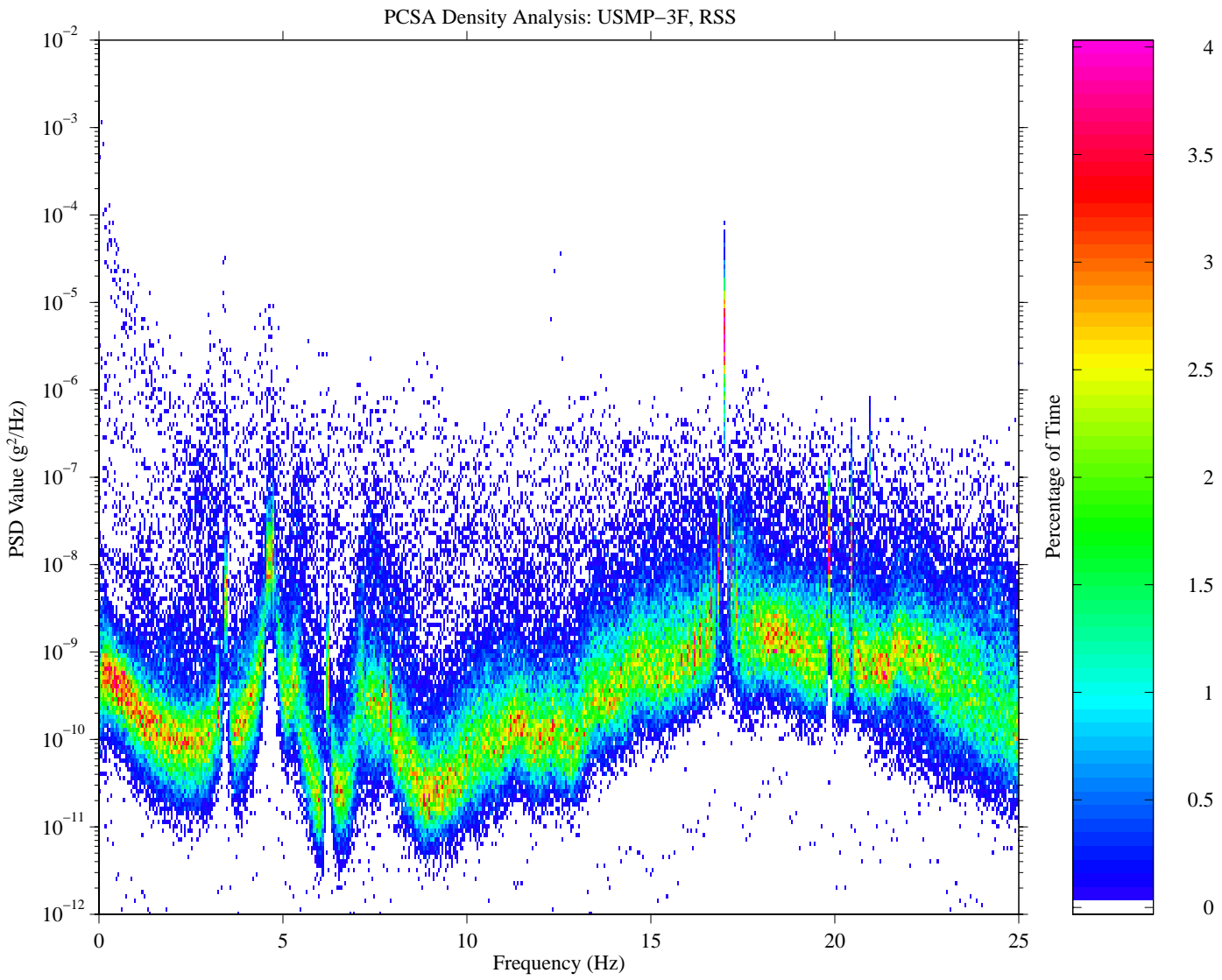


Figure 11: PCSA plot for USMP-3 microgravity portion of STS-75

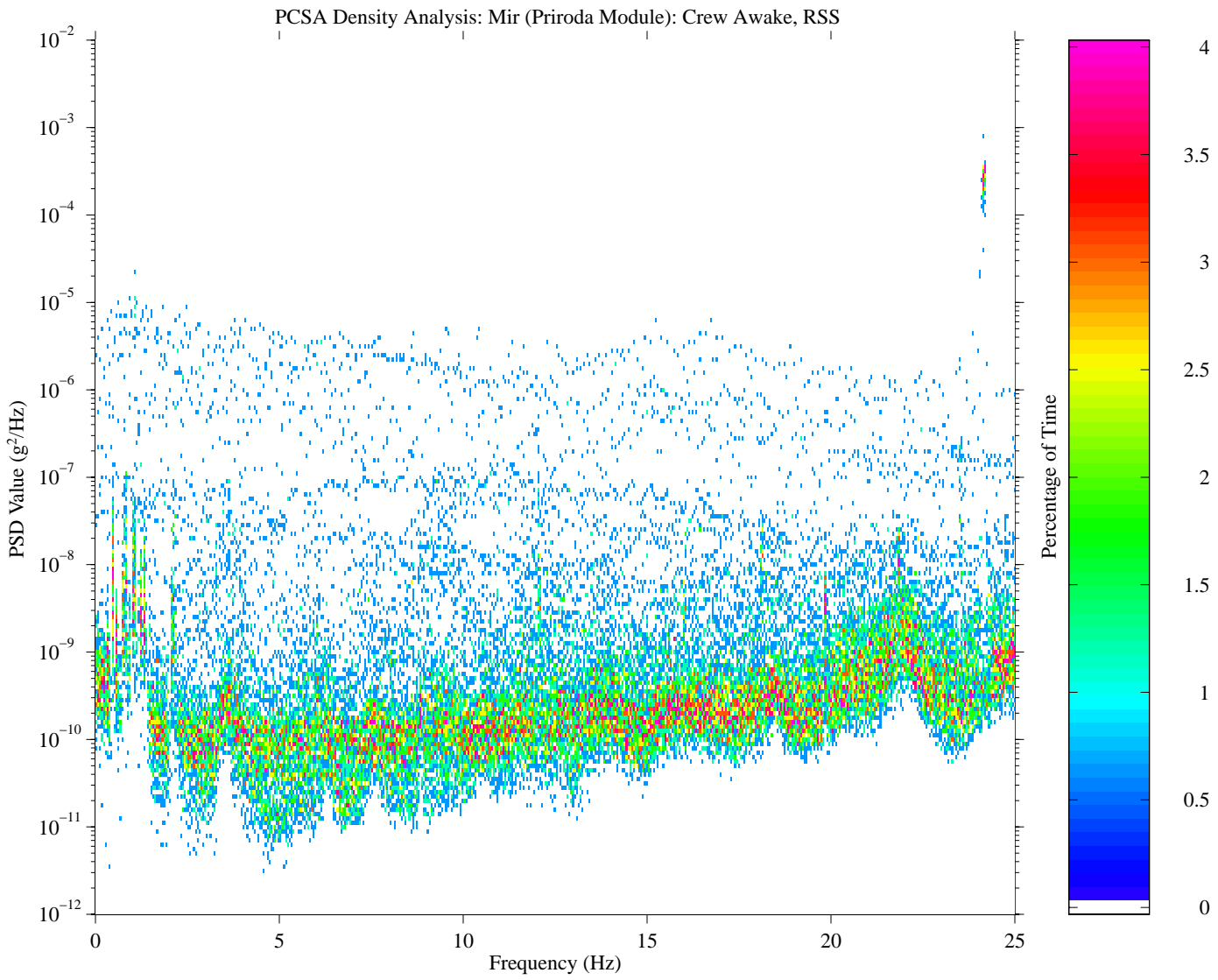


Figure 12: PCSA plot for crew active on Mir space station

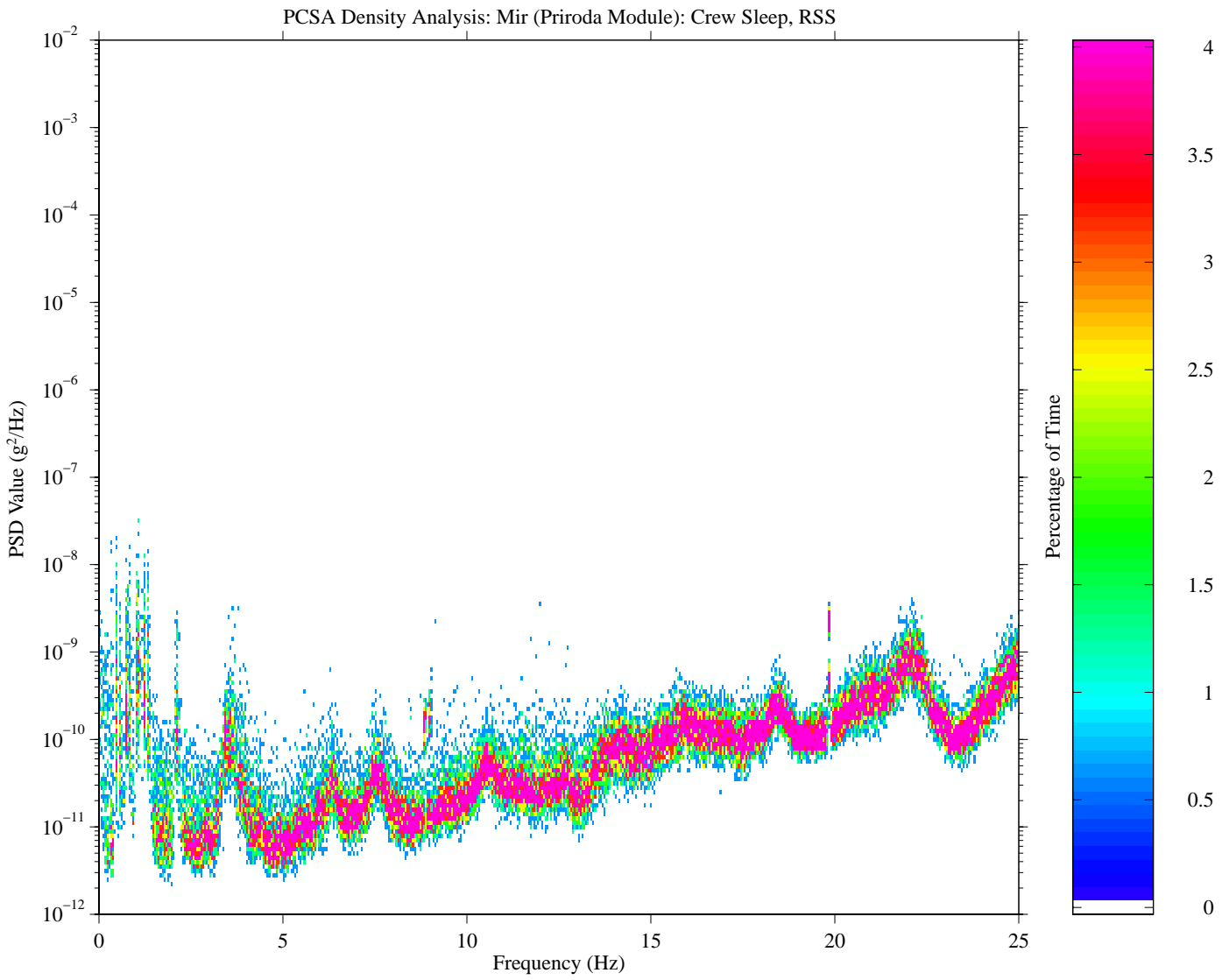
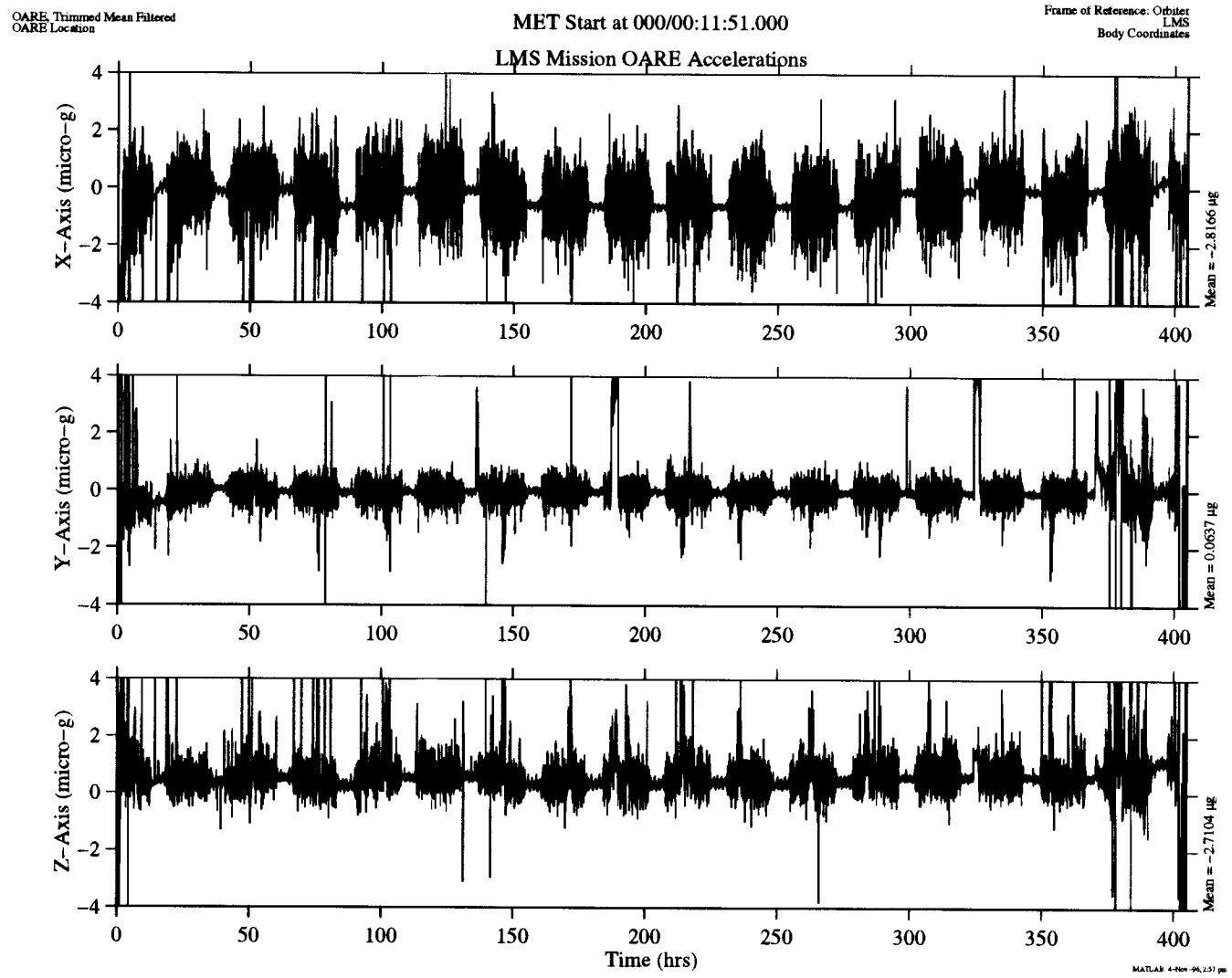


Figure 13: PCSA plot for crew rest on Mir space station

Figure 14: OARE sampled data set in acceleration vs. time for STS-78 / LMS



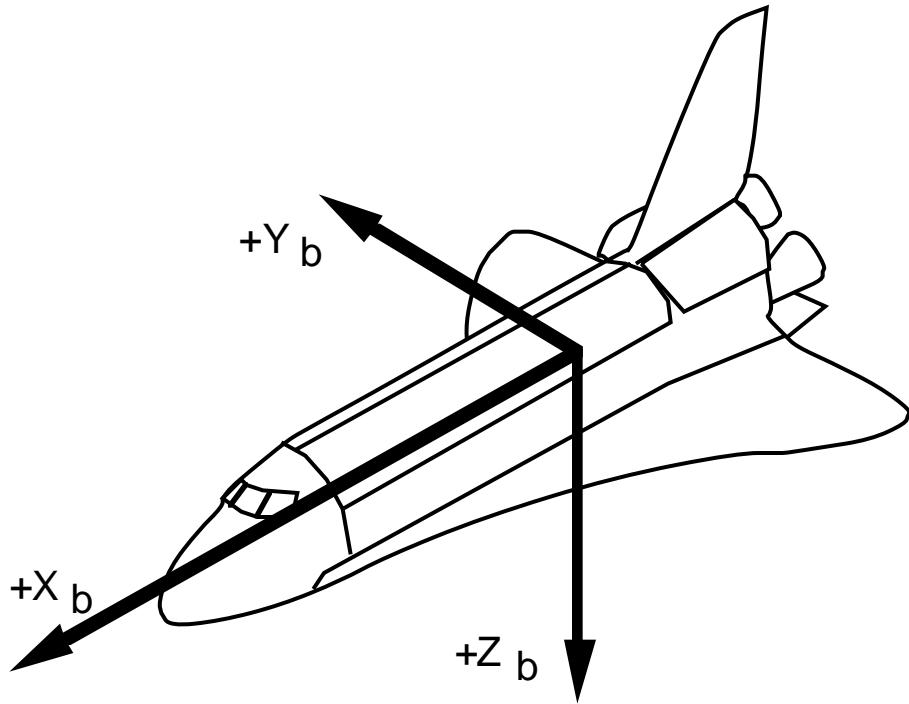


Figure 15: Orbiter body axes coordinate system

Figure 16: Typical Quasi-steady Three-dimensional Histogram (STS-78 / LMS)

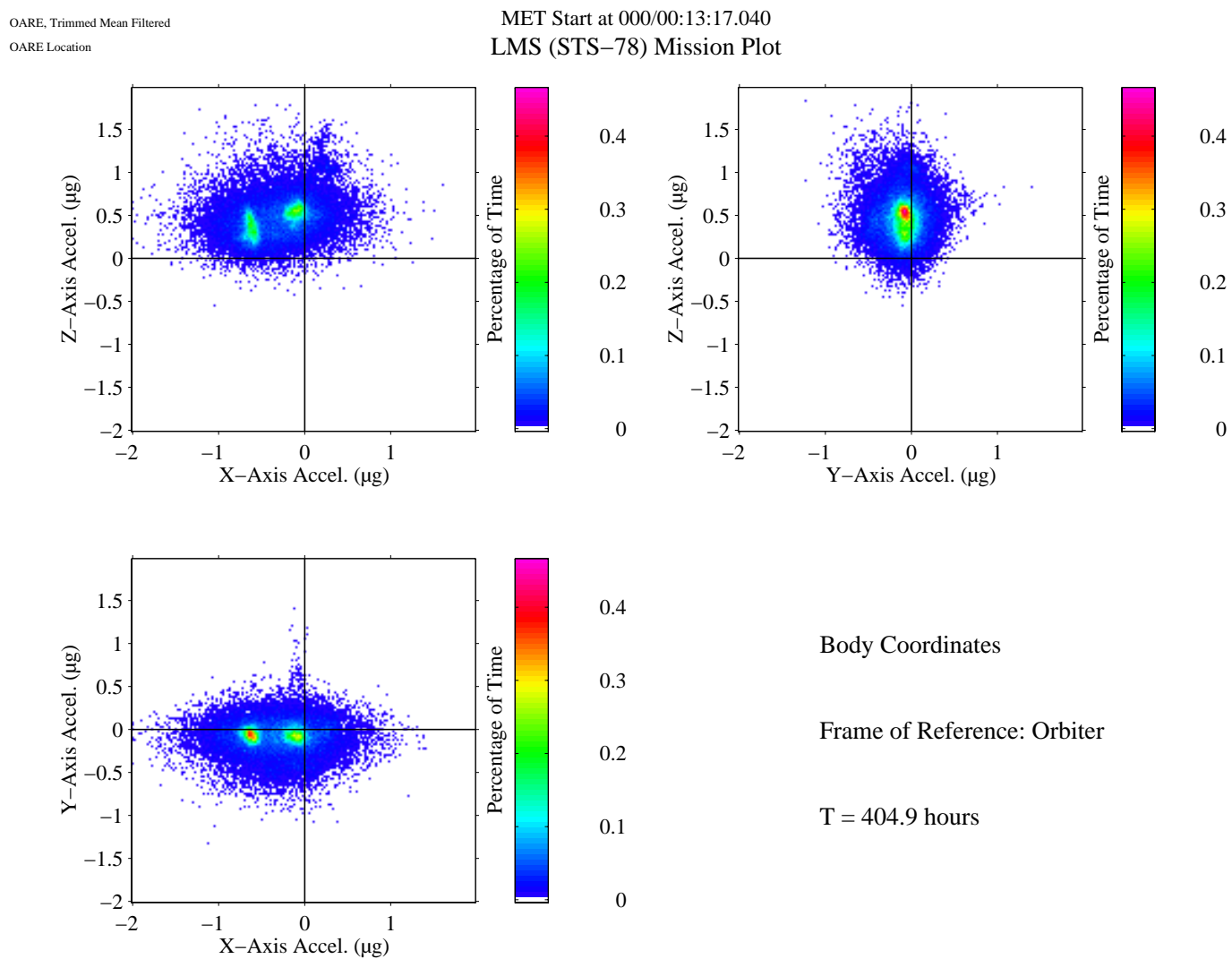


Figure 17: QTH plot for entire STS-62 mission

OARE, Trimmed Mean Filtered  
OARE Location

MET Start at 000/00:12:16.920  
USMP-2 (STS-62) Mission Plot

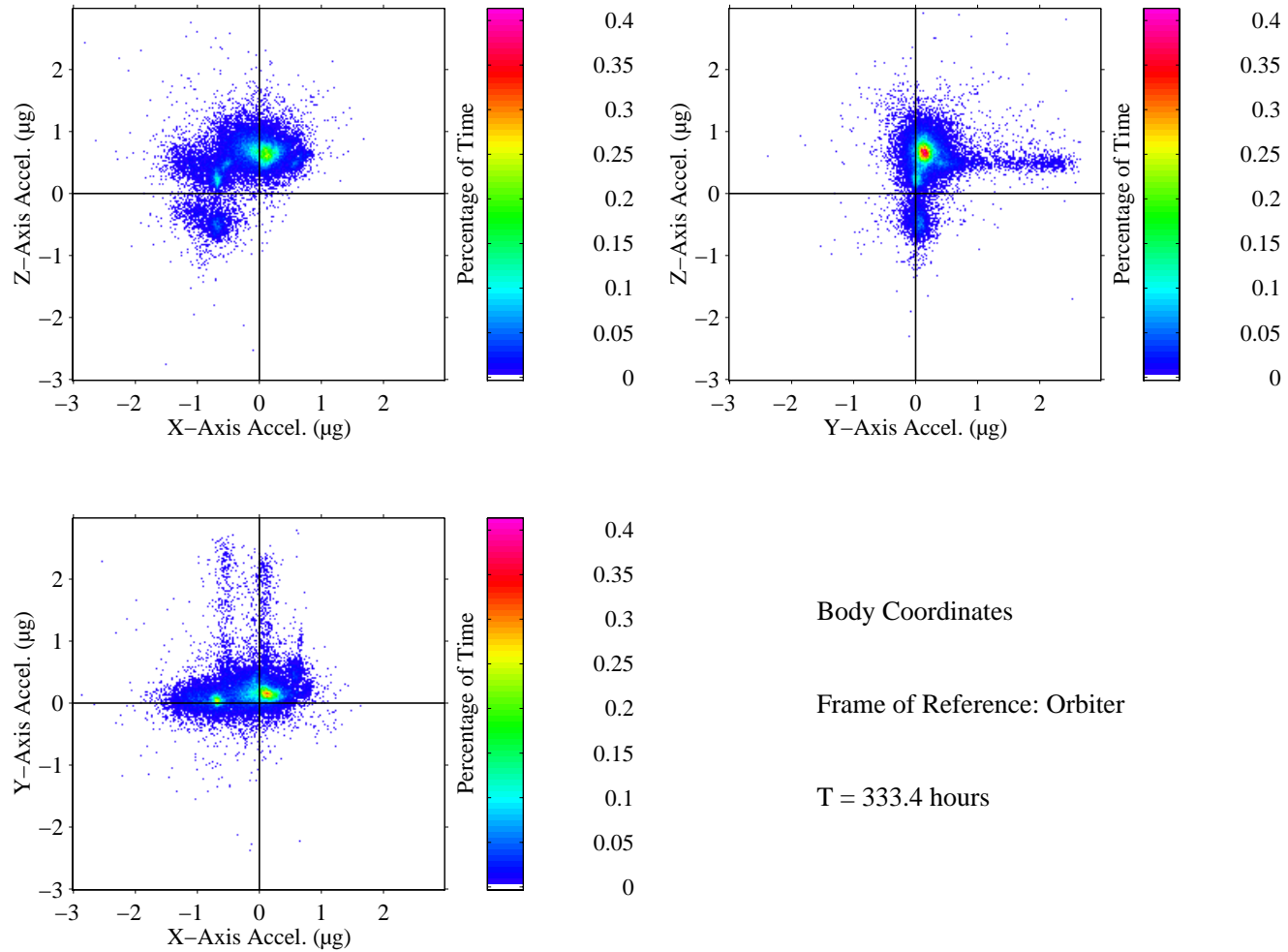


Figure 18: QTH plot for USMP-2 microgravity time of STS-62

OARE, Trimmed Mean Filtered

OARE Location

MET Start at 000/00:12:16.920  
USMP-2 Microgravity Period

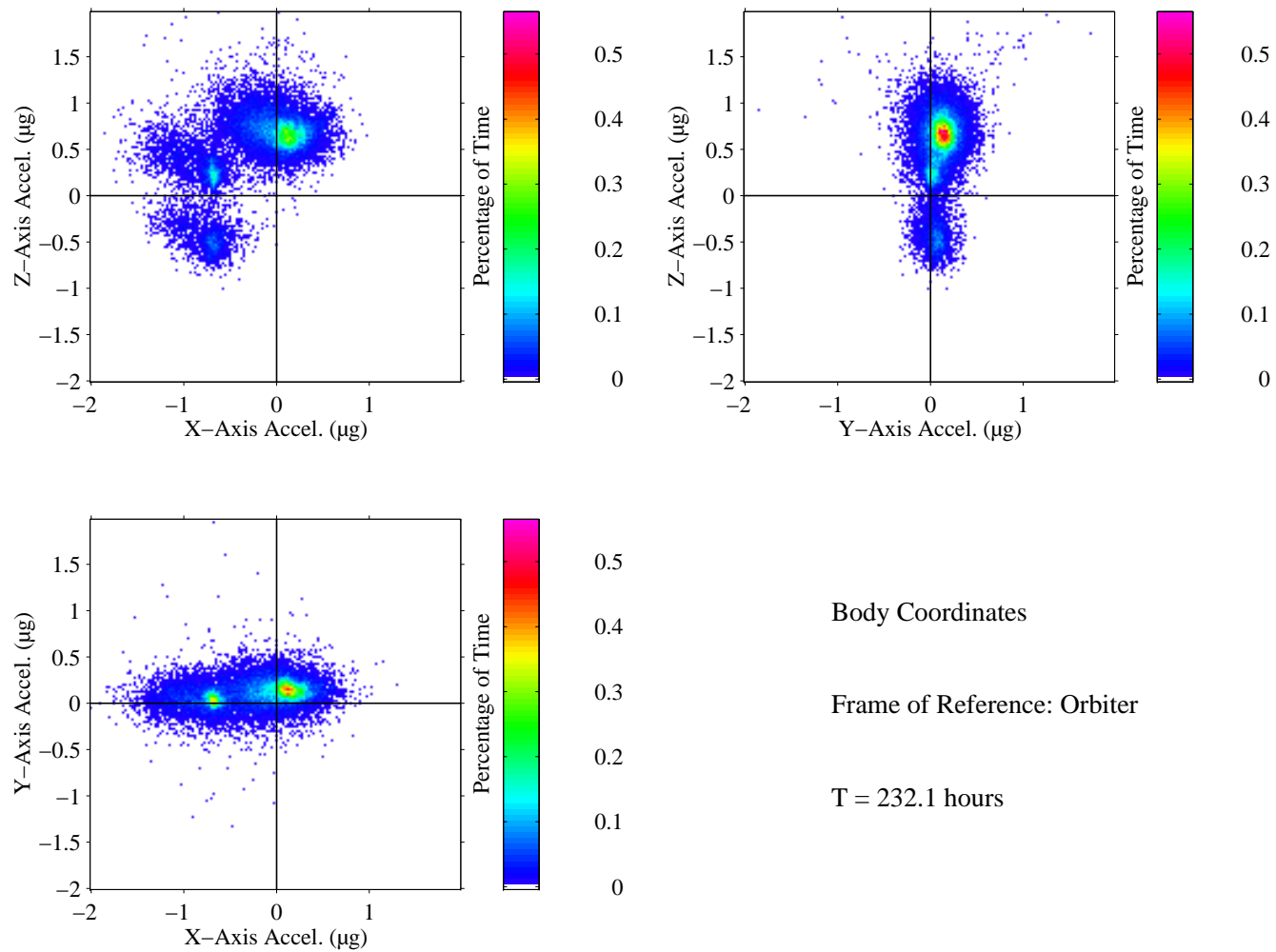
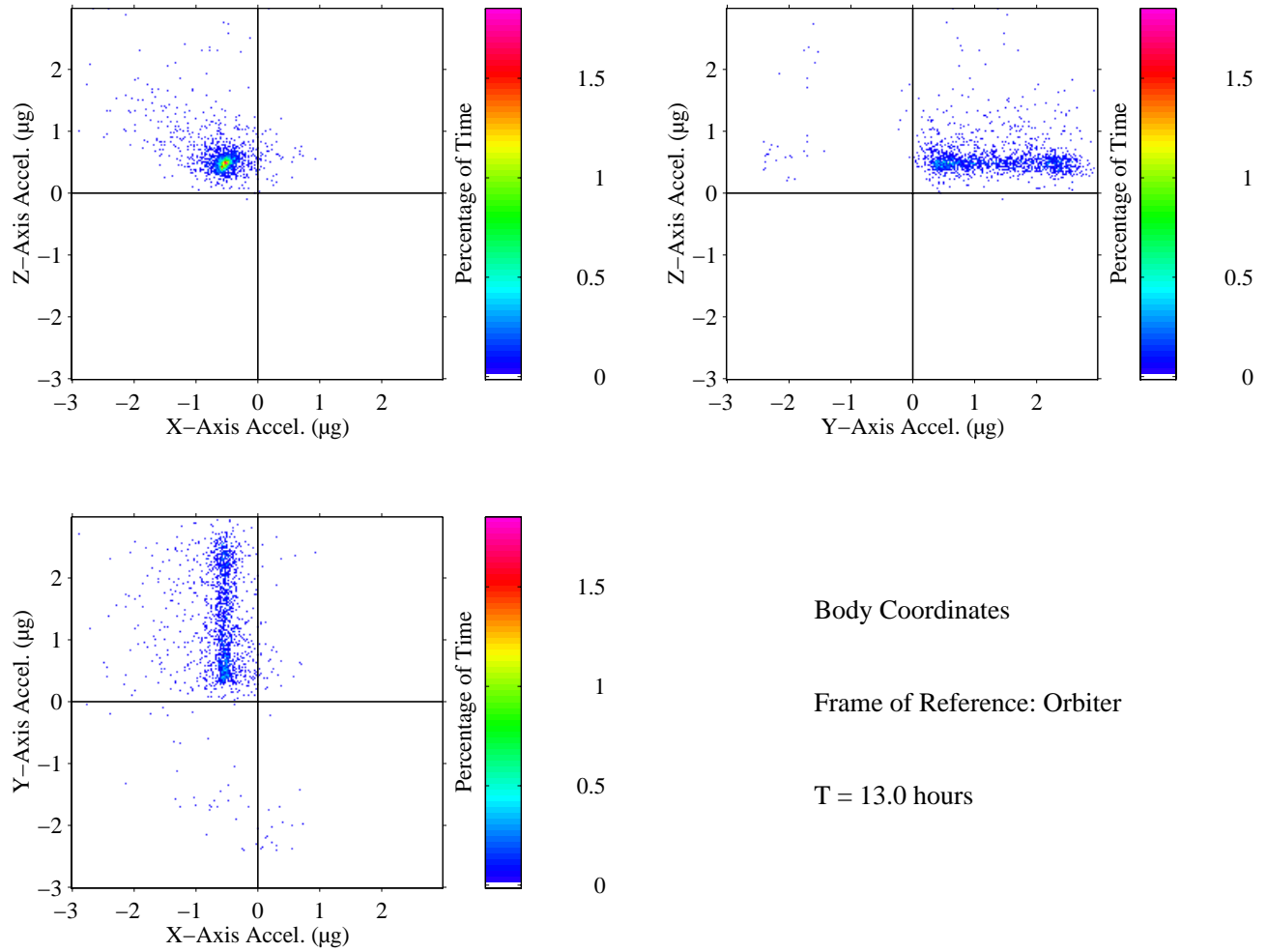


Figure 19: QTH plot during STS-62 with elliptical orbit parameters

OARE, Trimmed Mean Filtered  
OARE Location

MET Start at 013/04:00:02.880  
USMP-2 Elliptical Orbit



Body Coordinates

Frame of Reference: Orbiter

T = 13.0 hours

Figure 20: QTH plot for -ZLV/+YVV attitude during STS-62

OARE, Trimmed Mean Filtered  
OARE Location

MET Start at 000/11:00:07.920  
USMP-2 (STS-62) -ZLV/+YVV Attitude

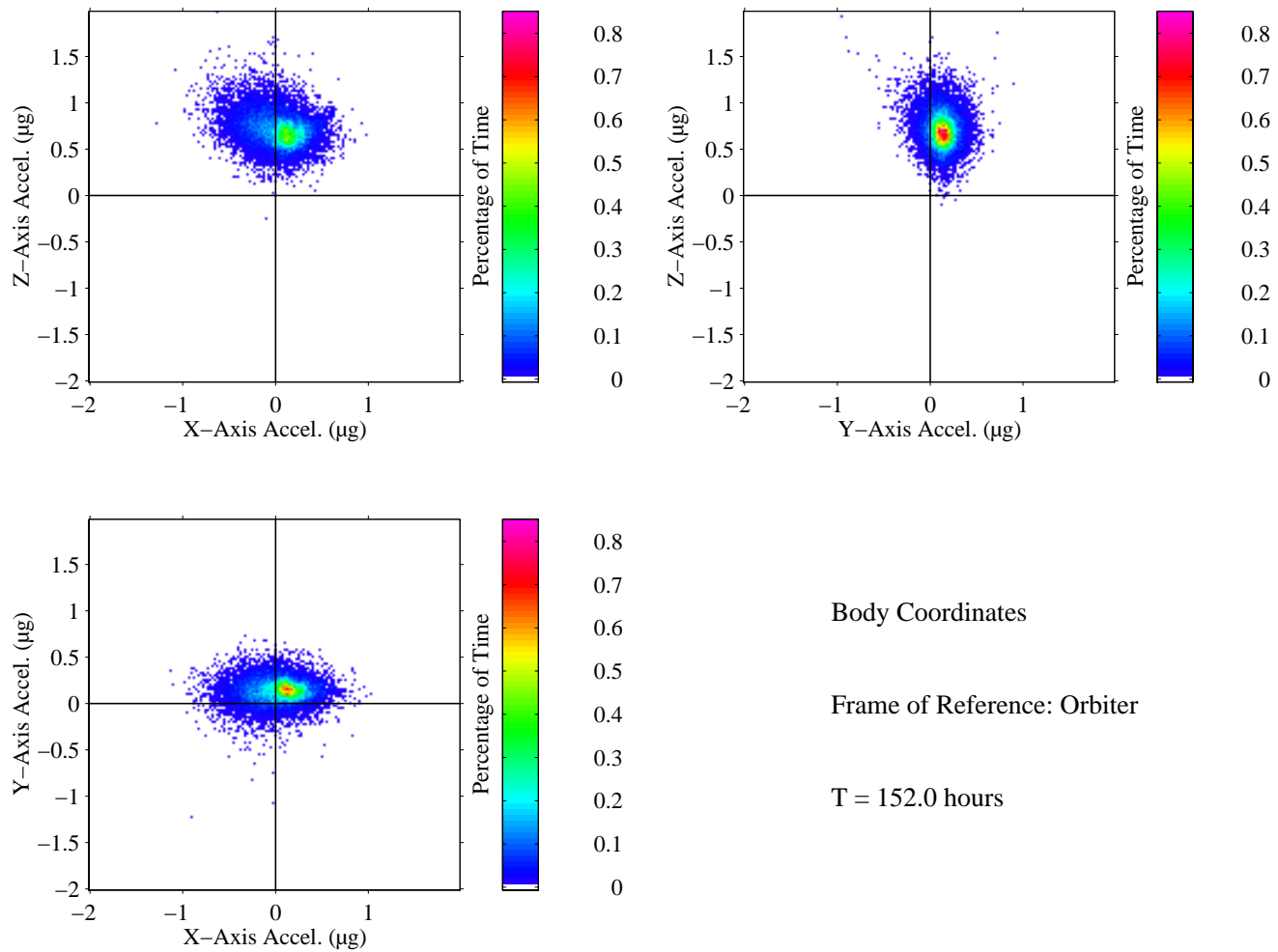


Figure 21: QTH plot for -XIV/-ZVV attitude during STS-62

OARE, Trimmed Mean Filtered

OARE Location

MET Start at 006/20:00:02.880  
USMP-2 (STS-62) -XIV/-ZVV Attitude

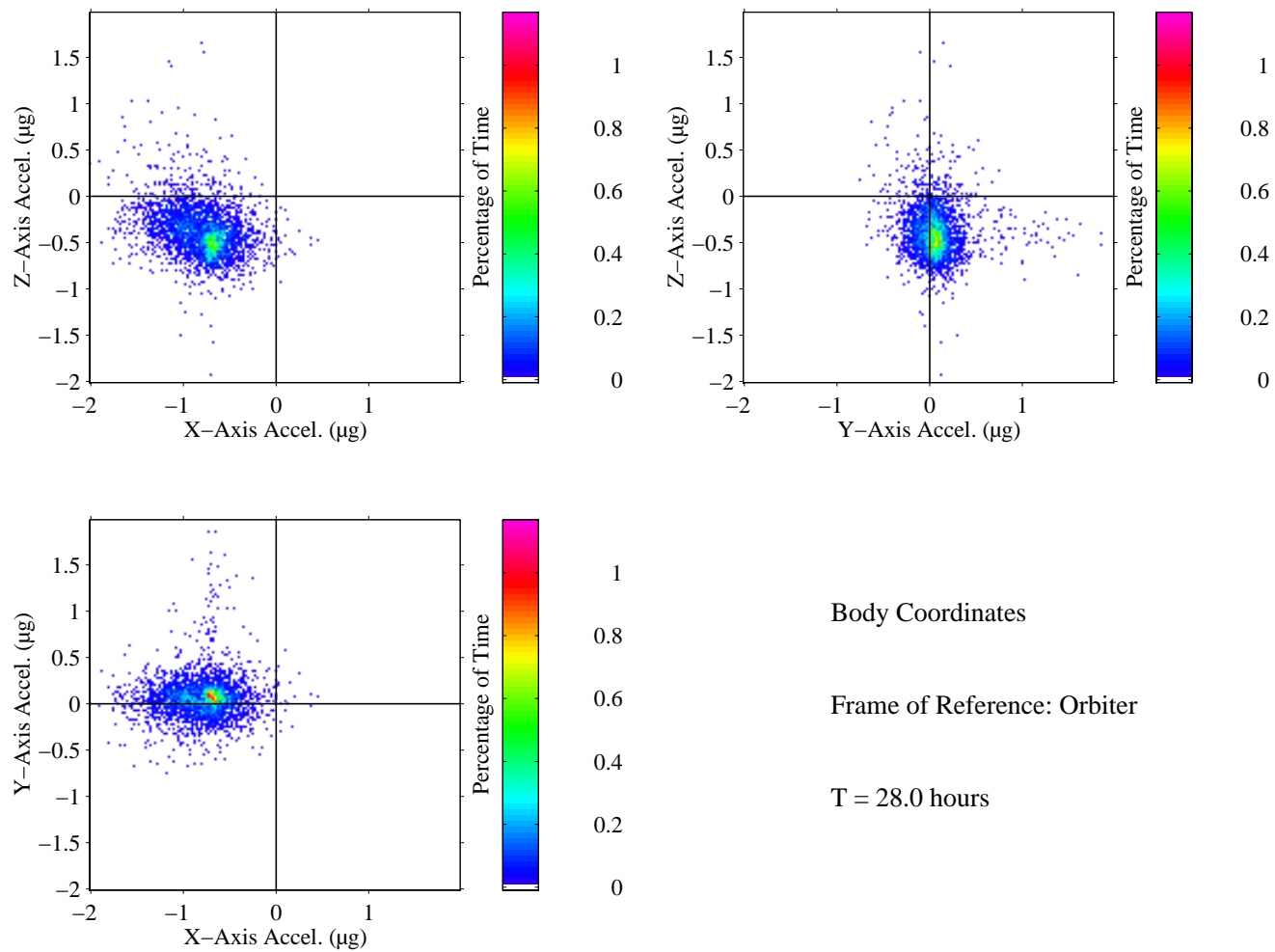
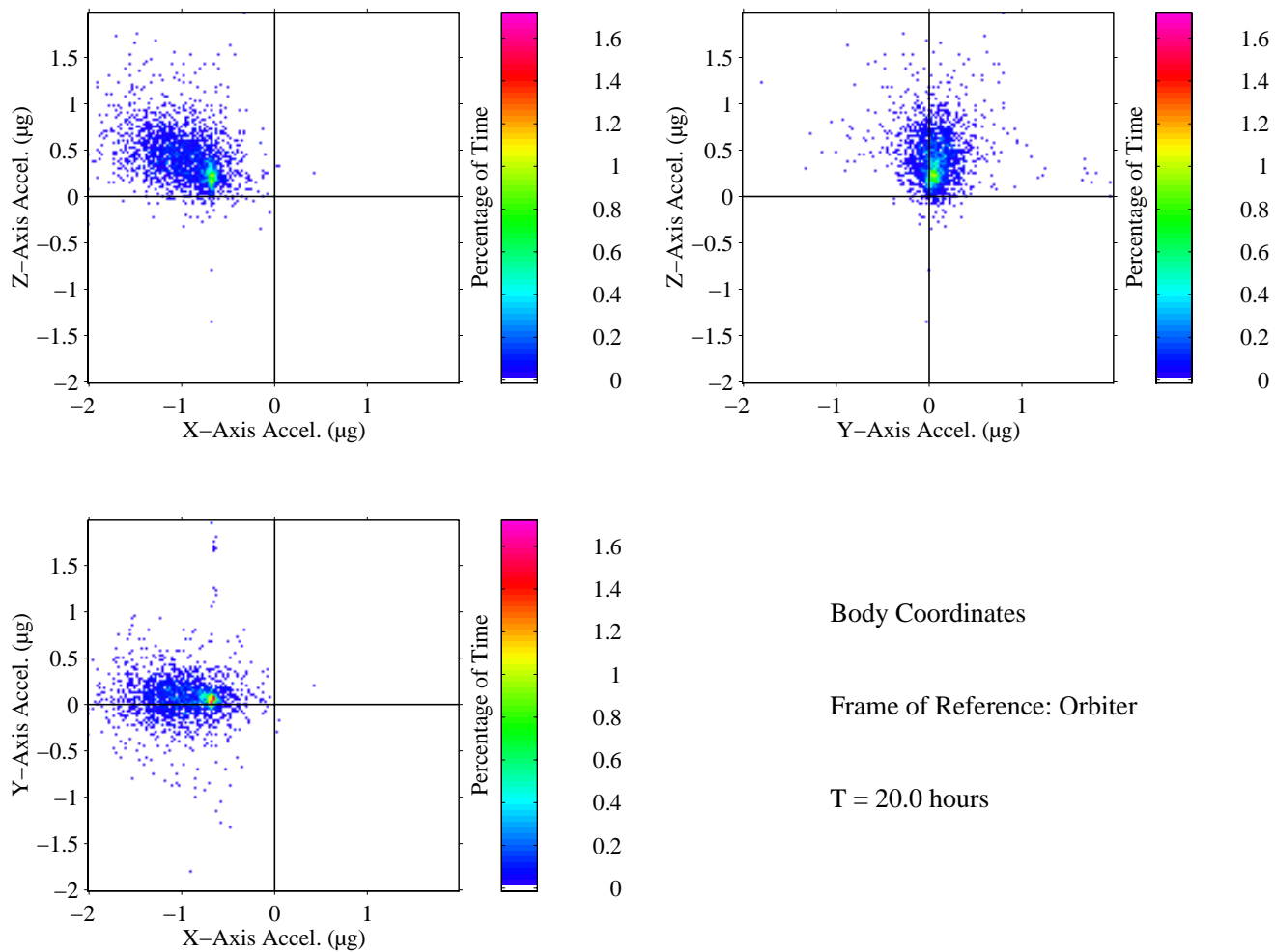


Figure 22: QTH plot for -XIV/+ZVV attitude during STS-62

OARE, Trimmed Mean Filtered  
OARE Location

MET Start at 008/01:00:02.880  
USMP-2 (STS-62) -XIV/+ZVV Attitude



Body Coordinates

Frame of Reference: Orbiter

T = 20.0 hours

Figure 23: QTH plot for crew active periods of STS-78 / LMS

OARE, Trimmed Mean Filtered  
OARE Location

MET Start at 008/17:00:16.920  
LMS Mission – Crew Active Periods

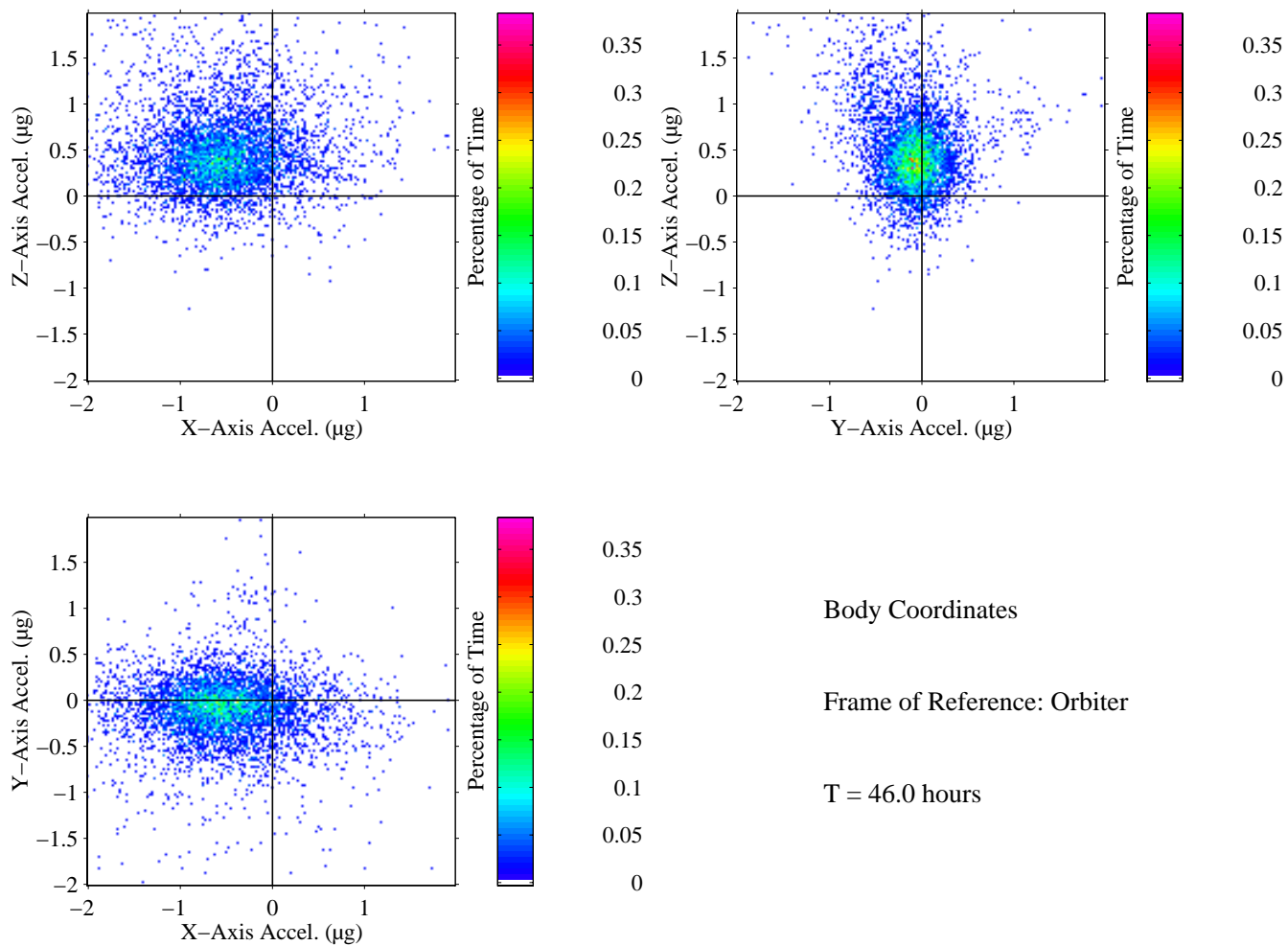
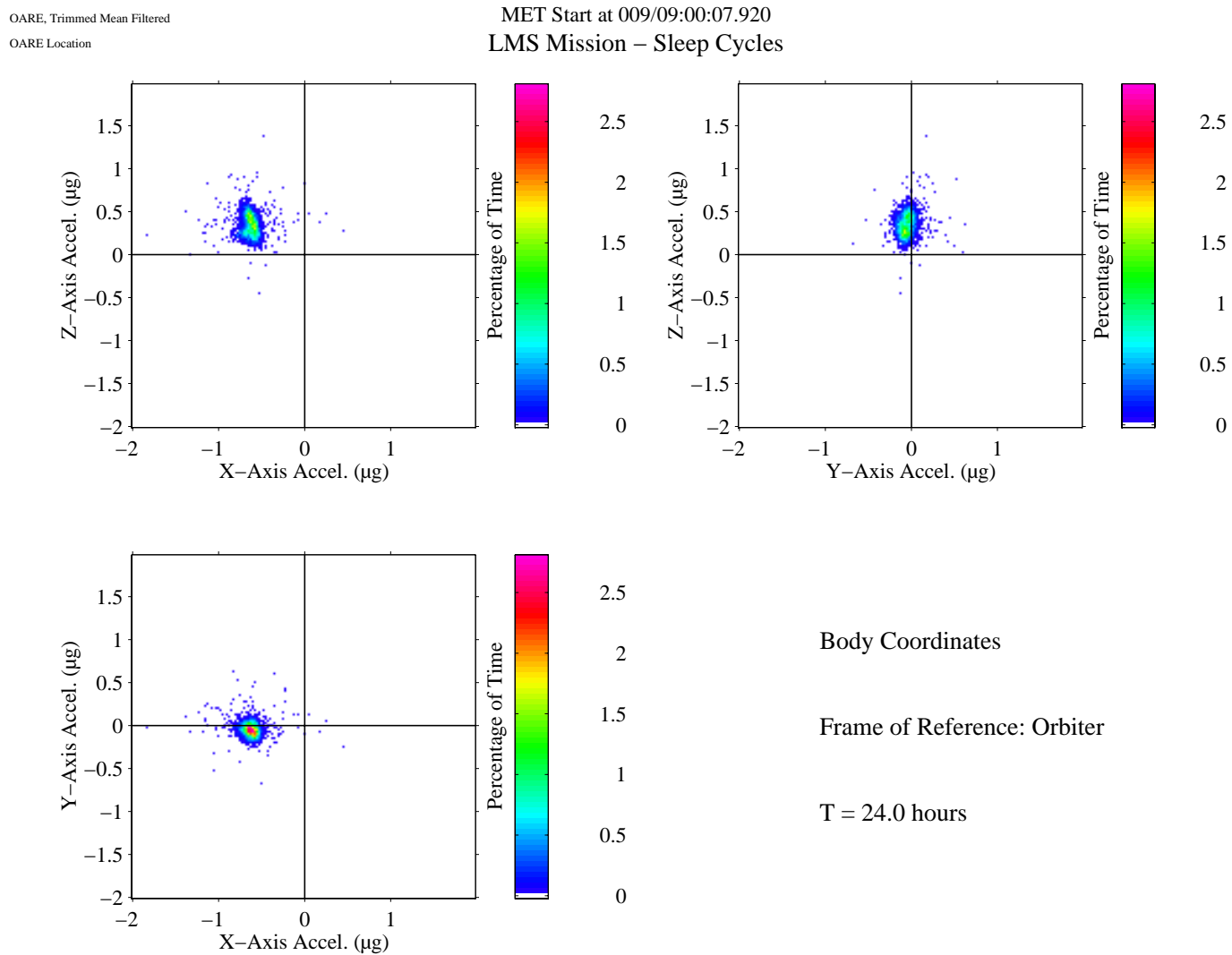


Figure 24: QTH plot for crew rest periods of STS-78 / LMS



# REPORT DOCUMENTATION PAGE

*Form Approved*  
OMB No. 0704-0188

Public reporting burden for this collection of information is estimated to average 1 hour per response, including the time for reviewing instructions, searching existing data sources, gathering and maintaining the data needed, and completing and reviewing the collection of information. Send comments regarding this burden estimate or any other aspect of this collection of information, including suggestions for reducing this burden, to Washington Headquarters Services, Directorate for Information Operations and Reports, 1215 Jefferson Davis Highway, Suite 1204, Arlington, VA 22202-4302, and to the Office of Management and Budget, Paperwork Reduction Project (0704-0188), Washington, DC 20503.

<b>1. AGENCY USE ONLY</b> ( <i>Leave blank</i> )		<b>2. REPORT DATE</b> April 1997	<b>3. REPORT TYPE AND DATES COVERED</b> Technical Memorandum	
<b>4. TITLE AND SUBTITLE</b> Comparison Tools for Assessing the Microgravity Environment of Missions, Carriers and Conditions			<b>5. FUNDING NUMBERS</b>  WU-963-60-0D	
<b>6. AUTHOR(S)</b> Richard DeLombard, Kevin McPherson, Milton Moskowitz, and Ken Hrovat				
<b>7. PERFORMING ORGANIZATION NAME(S) AND ADDRESS(ES)</b> National Aeronautics and Space Administration Lewis Research Center Cleveland, Ohio 44135-3191			<b>8. PERFORMING ORGANIZATION REPORT NUMBER</b>  E-10719	
<b>9. SPONSORING/MONITORING AGENCY NAME(S) AND ADDRESS(ES)</b> National Aeronautics and Space Administration Washington, DC 20546-0001			<b>10. SPONSORING/MONITORING AGENCY REPORT NUMBER</b>  NASA TM-107446	
<b>11. SUPPLEMENTARY NOTES</b> Richard DeLombard and Kevin McPherson, NASA Lewis Research Center; Milton Moskowitz and Ken Hrovat, Tal-Cut, Company, 24831 Lorain Road, Suite 203, North Olmsted, Ohio 44070 (work funded by NASA Contract NAS34-27254). Responsible person, Richard DeLombard, organization 6727, (216) 433-3285.				
<b>12a. DISTRIBUTION/AVAILABILITY STATEMENT</b>  Unclassified - Unlimited Subject Categories 20, 35, and 18  This publication is available from the NASA Center for AeroSpace Information, (301) 621-0390.			<b>12b. DISTRIBUTION CODE</b>	
<b>13. ABSTRACT</b> ( <i>Maximum 200 words</i> )  The Principal Component Spectral Analysis and the Quasi-steady Three-dimensional Histogram techniques provide the means to describe the microgravity acceleration environment of an entire mission on a single plot. This allows a straight forward comparison of the microgravity environment between missions, carriers, and conditions. As shown in this report, the PCSA and QTH techniques bring both the range and median of the microgravity environment onto a single page for an entire mission or another time period or condition of interest. These single pages may then be used to compare similar analyses of other missions, time periods or conditions. The PCSA plot is based on the frequency distribution of the vibrational energy and is normally used for an acceleration data set containing frequencies above the lowest natural frequencies of the vehicle. The QTH plot is based on the direction and magnitude of the acceleration and is normally used for acceleration data sets with frequency content less than 0.1 Hz. Various operating conditions are made evident by using PCSA and QTH plots. Equipment operating either full or part time with sufficient magnitude to be considered a disturbance is very evident as well as equipment contributing to the background acceleration environment. A source's magnitude and/or frequency variability is also evident by the source's appearance on a PCSA plot. The PCSA and QTH techniques are valuable tools for extracting useful information from acceleration data taken over large spans of time. This report shows that these techniques provide a tool for comparison between different sets of microgravity acceleration data, for example different missions, different activities within a mission, and/or different attitudes within a mission. These techniques, as well as others, may be employed in order to derive useful information from acceleration data.				
<b>14. SUBJECT TERMS</b> Microgravity environment; SAMS; OARE; Orbiter; Mir; Acceleration measurements			<b>15. NUMBER OF PAGES</b> 41	
			<b>16. PRICE CODE</b> A03	
<b>17. SECURITY CLASSIFICATION OF REPORT</b> Unclassified	<b>18. SECURITY CLASSIFICATION OF THIS PAGE</b> Unclassified	<b>19. SECURITY CLASSIFICATION OF ABSTRACT</b> Unclassified	<b>20. LIMITATION OF ABSTRACT</b>	